CERES_SSF1deg-Hour/Day/Month_Ed4A
Data Quality Summary

Version 2
Updated 8/4/2023

Investigation: **CERES**
Data Products: **SSF1deg-Hour**
SSF1deg-Day/Month

Data Sets: **Terra, Aqua, NPP, NOAA-20**

Data Set Versions:	**Terra/Aqua Edition4A**	**Release Date: May 11, 2017**
	NPP Edition2A	**Release Date: April 5, 2022**
	NOAA-20 Edition1B	**Release Date: April 5, 2022**

CERES Visualization, Ordering and Subsetting Tool: https://ceres.larc.nasa.gov/data/

The purpose of this document is to inform users of the accuracy of this data product as determined by the CERES Science Team. The document summarizes key validation results, provides cautions where users might easily misinterpret the data, provides links to further information about the data product, algorithms, and accuracy, and gives information about planned data improvements.

This document is a high-level summary and represents the minimum information needed by scientists for appropriate and successful use of this data product. It is strongly suggested that authors, researchers, and reviewers of research papers re-check this document (especially Cautions and Helpful Hints) for the latest status before publication of any scientific papers using this data product.

TABLE OF CONTENTS

Section Page

1.0 Nature of the CERES_SSF1deg-Hour/Day/Month_Ed4A Products 1
2.0 CERES Processing Level and Product Description 3
3.0 Cautions and Helpful Hints 5
4.0 Version History 12
4.1 Changes Between the Initial and Revised Versions of SSF1deg Ed4A 12
4.2 Algorithm Changes Between SSF1deg Ed3A and SSF1deg Ed4A 16
4.3 Input Changes Between SSF1deg Ed3A and SSF1deg Ed4A 16
4.4 Ed4A Input Improvements over Ed3A 16
4.4.1 Terra Cloud Optical Depth 16
4.4.2 GEOS Versions 17
4.4.3 MODIS Land Aerosol Optical Depth 19
4.5 Ed4A Input Trend Anomalies 19
4.5.1 CERES Terra-MODIS Cloud Phase 19
4.5.2 CERES Terra-MODIS 1.2-μm Channel Cloud Properties 20
5.0 Accuracy and Validation 22
5.1 SSF1deg Ed4A Uncertainties 22
5.2 SSF1deg Ed4A and Ed3A Cloud and Flux Comparisons 22
5.3 Initial SSF1deg Ed4A Terra, Aqua, and NPP Comparisons 30
6.0 References 32
7.0 Expected Reprocessing 34
8.0 Attribution 35
9.0 Feedback and Questions 36
10.0 Appendix - The Calendar Year Anomaly Dilemma 37
11.0 Document Revision Record 40

LIST OF FIGURES

Figure Page

Figure 3-1. Terra and Aqua mean local equatorial crossing time (MLT) for January 2019 through July 2026. 6

Figure 3-2. TSIS-1 TIM Version 3 at 1 AU incorrect scaling (red daily values) compared to the correct scaling (black daily values). 8

Figure 4-1. The monthly regional all-sky SW initial minus revised SSF1deg Ed4A bias for (left panel) Terra and (right panel) Aqua for Jan. 2008, Apr. 2008, June 2008, and Nov. 2008. The revised Ed4A (empirical Ed4A snow and ice directional models) is considered more accurate than the initial version (theoretical TRMM directional models). The bias scale is shown between the June 2008 and Nov. 2008 plots; units are W m^{-2}. 13

Figure 4-2. The monthly global all-sky SW initial minus revised SSF1deg Ed4A bias for (top) Terra and (bottom) Aqua over their respective records. The revised Ed4A (empirical Ed4A snow and ice directional models) is considered more accurate than the initial version (theoretical TRMM directional models). 14

Figure 4-3. The monthly regional clear-sky SW initial minus revised SSF1deg Ed4A bias for June 2008 for both Terra (left) and Aqua (right). Units are W m^{-2}. 15

Figure 4-4. The monthly regional ocean coverage initial minus revised SSF1deg Ed4A bias for June 2008 for Terra. Units are percent. 15

Figure 4-5. Comparison of the SSF1deg Terra-MODIS global monthly mean optical depth (daytime only) between Ed4A and Ed3A. Note the Terra-MODIS C5 calibration anomalies during 2003 and 2009 for Ed3A are mitigated by Ed4A processing. 17

Figure 4-6. Comparison of the SSF1deg Aqua global monthly mean clear-sky LW TOA flux anomalies between Ed4A and Ed3A. Note the Ed3A discontinuity during January 2008 coincides with the transition between GEOS-4.0 and GEOS-5.2. GEOS-5.4.1 has been used over the entire Ed4A record. 18

Figure 4-7. Same as Figure 4-6 except for precipitable water (PW). 18

Figure 4-8. Comparison of the Terra-MODIS global monthly mean land aerosol optical depth at 0.55 μm between Ed4A and Ed3A. Note the Ed3A discontinuity during April 2006 coincides with the transition between MODIS Collections 4 and 5. 19

LIST OF FIGURES

Figure Page

Figure 4-9. The Terra SSF1deg Ed4A global monthly mean cloud phase for (top) day-only and (bottom) day and night. Cloud phase of 1 indicates liquid cloud and 2 indicates ice. The cloud phase did not have a trend in Ed3A. 20

Figure 4-10. The Terra SSF1deg Ed4A global monthly mean cloud optical depth (top), ice particle size (middle), and liquid particle size (bottom) for daytime only based on the Terra-MODIS 1.2-μm channel. Units of particle size are μm. 21

Figure 5-1. (left panels) The regional monthly mean total cloud fraction (%) for SSF1deg Ed4A and (right panels) for SSF1deg Ed4A minus Ed3A for (top row) Terra Jan. 2010, (2nd row) Terra July 2010, (3rd row) Aqua Jan. 2010, and (bottom row) Aqua July 2010. 23

Figure 5-2. The SSF1deg Ed4A minus Ed3A global monthly mean day/night total cloud fraction (%) for (top) Terra and (bottom) Aqua. 24

Figure 5-3. The Terra 2003-2015 13-year regional means of (left panel) SSF1deg Ed4A and (right panel) Ed4A minus Ed3A for (top row) all-sky SW flux, (2nd row) all-sky SW flux trend, (3rd row) all-sky LW flux, and (bottom row) all-sky LW flux trend. Unit of flux is W m^{-2}; unit of flux trend is W m^{-2} yr^{-1} 26

Figure 5-4. Same as Figure 5-3, except for Aqua. 27

Figure 5-5. The global monthly mean SSF1deg Ed4A minus Ed3A for (top panel) Terra all-sky SW flux, (2nd panel) Terra all-sky LW flux, (3rd panel) Aqua all-sky SW flux, and (bottom panel) Aqua all-sky LW flux. Units in W m^{-2}. 28

Figure 5-6. The 2003-2015 13-year regional means of (left panel) SSF1deg Ed4A and (right panel) Ed4A minus Ed3A for (top row) Terra clear-sky SW flux, (2nd row) Terra clear-sky LW flux, (3rd row) Aqua clear-sky SW flux, and (bottom row) Aqua clear-sky LW flux. Units in W m^{-2} 29

Figure 10-1. (left) The Earth's declination angle (deg), (middle) Earth-sun distance correction factor, and (right) sidereal day angle or equation of time (deg) as a function of day of year. 37

Figure 10-2. (left) The monthly SSF1deg Ed4A total solar incoming (TSI) irradiance anomaly based on the calendar year (black line) and the monthly SORCE TSI anomaly after subtracting the record mean (red line). (right) The theoretical monthly TSI anomaly based on a solar constant of 1361 W m^{-2} and the calendar year. Units in W m^{-2}. 38

Figure 10-3. The SSF1deg Ed4A zonal monthly TSI anomalies for 4 latitude zones. Units in W m^{-2}. 38

LIST OF TABLES

Table Page

Table 2-1. CERES processing level descriptions. 3

Table 3-1. Dates of the major data gaps in the Terra and Aqua CERES records. 5

Table 3-2. Dates of the major data gaps in the NPP and NOAA-20 CERES records. 5

Table 3-3. CERES nested grid. 7

Table 3-4. The geodetic minus spherical earth annual global flux means. 9

Table 4-1. The MODIS and GEOS versions used in SSF1deg Ed3A and Ed4A. 16

Table 5-1. The 2003-2015 13-year global mean cloud amount (%), cloud optical depth, cloud phase (1.0=liquid, 2=ice), cloud effective temperature (K), and cloud IR emissivity for daytime (SZA<90°) and day/night (24-hour) MODIS cloud properties for CERES Terra and Aqua SSF1deg Ed3A and Ed4A data products 25

Table 5-2. The 2003-2015 13-year global mean TOA solar incoming (S_0), SW, LW and net fluxes (W m^{-2}) for all-sky and clear-sky from CERES Terra and Aqua SSF1deg Ed3A and Ed4A. 30

Table 5-3. The December 2012 to November 2015 3-year global mean TOA solar incoming (S_0), SW, LW and net fluxes (W m^{-2}) for all-sky and clear-sky from CERES Terra and Aqua SSF1deg Ed4A and NPP SSF1deg Ed1A products. 31

Table 10-1. The annual Southern minus Northern Hemisphere TSI flux difference (W m^{-2}) as a function of a 365.25-day year and a calendar year. Note that 2004 is a leap year with 366 days. 39

Table 10-2. The monthly weighted minus daily weighted global annual SW, LW, and solar incoming flux (W m^{-2}). Note that 2004 and 2008 are leap years. 39

1.0 Nature of the CERES_SSF1deg-Hour/Day/Month_Ed4A Products

The CERES SSF1deg-Hour/Day/Month products provide 1°-regional gridded instantaneous (hour), daily and monthly averaged top of the atmosphere (TOA) radiative fluxes and associated MODIS-derived cloud properties from the observed instantaneous footprint SSF Ed4A fluxes and clouds. The regional monthly mean parameters are also zonally and globally averaged. TOA fluxes are provided for clear-sky and all-sky conditions for longwave (LW), shortwave (SW), and window (WN) wavelength bands. The cloud properties are averaged for both day/night (24-hour) and day-only time periods. Cloud properties are stratified into 4 atmospheric layers (surface-700 hPa, 700 hPa-500 hPa, 500 hPa-300 hPa, 300 hPa-tropopause) and provided for the total layer as well. The NASA-GSFC Global Modeling and Assimilation Office (GMAO) Goddard Earth Observing System (GEOS) version 5.4.1 provides the atmospheric profiles (Rienecker et al. 2008). The snow and ice daily coverage is from the NSIDC (National Snow and Ice Data Center) Near-Real-Time SSM/I-SSMIS EASE-Grid Daily Global Ice Concentration and Snow Extent product. The aerosols are from the NASA-GSFC MODIS MOD04_L2/MYD04_L2 products (Remer et al. 2005) and MATCH Aerosol Transport Model constituents (Collins et al. 2001). The incoming solar daily irradiance is from the SORCE TSI [Solar Radiation and Climate Experiment, Total Solar Irradiance, (Kopp et al. 2005)]. The SSF1deg products are processed separately for each satellite. Although there are two CERES instruments on both Terra and Aqua and one instrument on NPP, only the instrument in cross-track mode is utilized. For Edition 4A there are Terra, Aqua, and NPP SSF1deg single satellite products.

The SSF footprint CERES fluxes and MODIS clouds are first spatially averaged into 1° gridded regions. The CERES footprint center latitude and longitude location assigns the region. The CERES SSF1deg-Hour product contains these flux and cloud instantaneous spatially gridded means. The instantaneous gridded means are organized in daily files and contain the regional data that fall within the CERES orbit swaths for the day.

The SSF1deg-Day and -Month products contain 1°-regional daily and monthly averaged fluxes and clouds. The SW radiative fluxes between CERES observation times are determined from scene-dependent diurnal albedo models, which describe how TOA albedo (and therefore flux) changes with solar zenith angle for each local time while assuming the scene properties remain invariant throughout the day. These models are based upon the CERES Angular Distribution Models (ADMs) developed for the Tropical Rainfall Measuring Mission (TRMM) satellite (Loeb et al. 2003). The temporal averaging approach assumes constant meteorology throughout the day where the SW flux is determined by the variation of solar zenith angle given the cloud properties at the time of observation. The LW fluxes in between CERES observations are assumed to vary linearly over oceans, while daytime and nighttime observations over land and desert are interpolated by fitting a half-sine curve to the observations to account for the much stronger diurnal cycle over land and desert, similar to the ERBE methodology (Young et al. 1998). Due to the sparseness of observed clear-sky LW fluxes, the clear-sky LW flux *over land* is determined by applying the half-sine curve using all available clear-sky observations during the month. The SW and LW daily and monthly means are then the average of the hourly incremented fluxes whether observed or diurnally modeled.

The daily and monthly mean cloud properties are determined as follows. The MODIS pixels contained in the CERES footprint (nominal 20-km) are aggregated into clear-sky and two dynamic cloud layers in the SSF product. The instantaneous footprint cloud properties are then spatially averaged into 1° regions with 4 static cloud layers, which are stratified between the surface, 700 hPa, 500 hPa, 300 hPa and 50 hPa, as determined by the effective pressure. The daily and monthly averaged clouds are based on hourly observed and temporally interpolated clouds. The cloud properties are temporally interpolated as follows. The instantaneous regional observed cloud properties are placed into the appropriate hour-box and are then linearly interpolated to fill in the remaining hour-boxes. The hour-box cloud layer properties are then averaged into monthly means by weighting by cloud layer fraction. Similarly, the monthly mean total cloud properties are obtained by averaging the individual cloud layer monthly means. The daytime cloud properties are obtained from day-time hour-boxes where the solar zenith is less than 90°. Day/night (24-hour) cloud properties are computed using all hour-boxes for the day or month. Cloud optical depth is averaged in log form, since log cloud optical depth is proportional to visible radiance. Liquid water path (LWP) and ice water path (IWP) are computed hourly from cloud optical depth and particle radius for consistency. Similarly to clouds, atmospheric properties, aerosols, and snow and ice coverage are temporally interpolated linearly to determine the daily and monthly averages.

The SSF1deg-Month product also contains zonal and global fluxes, clouds, and atmospheric parameters. The zonal fluxes are the mean of all regional fluxes for each 1°-latitude zone. The global flux is derived by area-weighting the zonal fluxes based on oblate spheroid geometry. CERES can only measure fluxes for solar zenith angles less than 86°. For polar latitudes where the solar incoming flux is greater than zero, but where no CERES SW fluxes are observed, the last valid observed albedo is extrapolated to the terminator latitude. The zonal SW flux is then calculated as the extrapolated albedo multiplied by the zonal solar irradiance.

We urge users to visit the CERES Data subsetting/visualization/ordering tool, which provides an improved user interface and a wider range of data formats (e.g., ASCII, netCDF); the Earthdata Search ordering tool is limited to HDF.

https://ceres.larc.nasa.gov/data/

2.0 CERES Processing Level and Product Description

This section explains the CERES processing flow from level 0 to level 3 products; the steps are summarized in Table 2-1. This section also briefly describes all of the publicly available CERES products and their processing differences to help the user find the appropriate product for their application.

Table 2-1. CERES processing level descriptions.

Level	Description	Data Product
0	Raw digitized instrument data for all engineering and science data streams in Consultative Committee for Space Data Systems (CCSDS) packet format.	
1B	Instantaneous filtered broadband radiances at the CERES footprint resolution, geolocation and viewing geometry, solar geometry, satellite position and velocity, and all raw engineering and instrument status data.	BiDirectional Scans (BDS)
2	Instantaneous geophysical variables at the CERES footprint resolution. Includes some Level 1B parameters and retrieved or computed geophysical variables (e.g., filtered and unfiltered radiances, viewing geometry, radiative fluxes, imager cloud and aerosol properties).	SSF
3	Radiative fluxes and cloud properties spatially averaged onto a uniform grid. Includes either instantaneous averages sorted by GMT hour or temporally interpolated averages at 1–hourly, daily, monthly or monthly hourly.	SSF1deg-Hour SSF1deg-Day, -Month SYN1deg-Hour, -Day, -MHour, -Month
3B	Level 3 data products adjusted within their range of uncertainty to satisfy known constraints (e.g., consistency between average global net TOA flux imbalance and ocean heat storage).	EBAF-TOA EBAF-Surface

CERES instruments fly on the Terra (descending sun-synchronous orbit with an equator crossing time of 10:30 A.M. local time) and Aqua or NPP (ascending sun-synchronous orbit with an equator crossing time of 1:30 P.M. local time) satellites. Each CERES instrument measures filtered radiances in the shortwave (SW; wavelengths between 0.3 and 5 μm), total (TOT; wavelengths between 0.3 and 200 μm), and window (WN; wavelengths between 8 and 12 μm) regions. Unfiltered SW, longwave (LW) and WN radiances are determined following Loeb et al. (2001). CERES instruments provide global coverage daily, and monthly mean regional fluxes are based upon complete daily samples over the entire globe.

Raw digitized instrument data (Level 0) are converted to instantaneous filtered radiances (Level 1) using the latest CERES gains (Thomas et al. 2010). Time-dependent spectral response function values are then used to correct for the imperfect spectral response of the instrument and convert

the filtered radiances into unfiltered SW, LW and WN radiances (Loeb et al. 2001; Loeb et al. 2016). Since there is no LW channel on CERES, LW daytime radiances are determined from the difference between the TOT and SW channel radiances. Instantaneous TOA radiative fluxes (Level 2) are estimated from unfiltered radiances using empirical ADMs (Su et al. 2015a) for different scene types identified using cloud property retrievals from MODIS measurements (Minnis et al. 2011). Their accuracy has been evaluated in several articles (Loeb et al. 2005 Loeb et al. 2007; Kato and Loeb 2005; Su et al. 2015b).

Monthly mean fluxes (Level 3) are determined by spatially averaging the instantaneous TOA flux values on a 1°×1° grid, temporally interpolating between observed values at 1-h increments for each hour of every month, and then averaging all hour boxes in a month (Doelling et al. 2013). CERES employs the CERES-only (CO; CERES SSF1deg stream) and the CERES-geostationary (CG; CERES SYN1deg stream) temporal interpolation methods. The CO method assumes that the cloud properties at the time of the CERES observation remain constant and only accounts for changes in albedo with solar zenith angle and diurnal land heating, by assuming a shape for unresolved changes in the diurnal cycle. The CG method enhances the CERES data by explicitly accounting for changes in clouds and radiation between CERES observation times using 1-hourly imager data from five geostationary (GEO) satellites that cover 60°S-60°N at any given time.

The Energy Balanced and Filled (EBAF, Level 3B) leverages off of the CERES Level 1-3 data products to produce a monthly TOA flux dataset that maintains the excellent radiometric stability of the CERES instruments while at the same time incorporating diurnal information from geostationary satellites in such a way as to minimize the impact of any geostationary imager artifacts that can occur over some geostationary domains and time periods. In order to ensure EBAF TOA fluxes satisfy known global mean energy budget constraints (e.g., based upon in-situ data from the Argo network, Roemmich et al. 2009), SW and LW TOA fluxes are adjusted within their range of uncertainty using an objective constrainment method (Loeb et al. 2009). Importantly, this is a one-time adjustment applied to the entire record. Therefore, the time-dependence of EBAF TOA fluxes is tied as closely as possible to the CERES instrument radiometric stability. Unlike other CERES data products, EBAF provides monthly regional clear-sky TOA fluxes that are free of missing regions by making optimal use of coincident CERES and MODIS measurements.

3.0 Cautions and Helpful Hints

The CERES Science Team notes several CAUTIONS and HELPFUL HINTS regarding the use of CERES_SSF1deg-Hour/Day/Month Ed4A:

- The CERES_SSF1deg Hour/Day/Month_Ed4.0 products can be visualized, subsetted, and ordered from: https://ceres.larc.nasa.gov/data/.
- There are occasional data gaps in the CERES observations. The major temporal data gaps are listed in Table 3-1 and Table 3-2. Also, small spatial data gaps occur over the equator where the CERES orbit swaths are not contiguous.

Table 3-1. Dates of the major data gaps in the Terra and Aqua CERES records.

Terra	Aqua
April 26-27, 2000	July 1-3, July 30-August 6, 2002
August 6-18, 2000	October 1-14, 2004 (instrument anomaly)
June 15-July 2, 2001	March 30-31, 2005
March 20-28, 2002	August 16-September 3, 2020
December 17-24, 2003	April 1-16, 2022
February 19-27, 2016	Drift begins March 1, 2023*
Drift begins July 1, 2022*	RAPS mode begins March 22, 2023**
October 11-23, 2022	

*When Terra and Aqua have drifted 15 minutes outside of their nominal 10:30AM and 1:30PM local equator crossing times and are slowly drifting towards the terminator.
**SSF1deg-Hour/Day/Month are not produced while instrument is in RAPS mode.

Table 3-2. Dates of the major data gaps in the NPP and NOAA-20 CERES records.

NPP	NOAA-20
RAPS mode August 19-31, 2019**	
RAPS mode October 1, 2019 onward**	

**SSF1deg-Hour/Day/Month are not produced while instrument is in RAPS mode.

- The CERES SSF1deg-Hour/Day/Month Ed4A are single satellite products. There is no SSF1deg product that combines measurements from multiple satellites. Only the CERES instrument that is in cross-track mode is used, since it provides uniform spatial distribution of footprints. No Rotating Azimuth Plane Scan (RAPS) is used**.** There are two CERES instruments on the Terra and Aqua satellites. All CERES Terra/Aqua instruments were calibrated to be on the same radiometric scale beginning with CERES Edition 3. For Terra, the FM1 instrument spends the most time in crosstrack mode. For Aqua, FM4 was the prime crosstrack instrument prior to March 2005, when the SW channel failed. After March 2005, Aqua FM3 was permanently placed in crosstrack mode. Only one CERES instrument, FM5, is onboard the NPP satellite, and it operates only in crosstrack mode until October 1, 2019. FM6 is on NOAA-20 and is in crosstrack mode. The CERES input data sources page (https://ceres.larc.nasa.gov/data/general-product-info/#ceres-input-data-sources) shows the Terra and Aqua instruments that are in cross-track mode.

- The Terra and Aqua orbits have started to drift towards their respective terminators, away their nominal 10:30AM and 1:30PM local equator crossing times. These satellites are expected to be de-orbited in early 2026. See Figure 3-1 for mean local equatorial crossing times as a function of year. Users are cautioned against determining trends with data during the drift period as the sampling time change of the regional diurnal cycles may be aliased into the long-term trends, especially in maritime stratus regions and land afternoon convection regions. See CERES Science Team Meeting presentation, pages 2-13: https://ceres.larc.nasa.gov/documents/STM/2022-10/Doelling_ERB_STM_oct2022.pdf

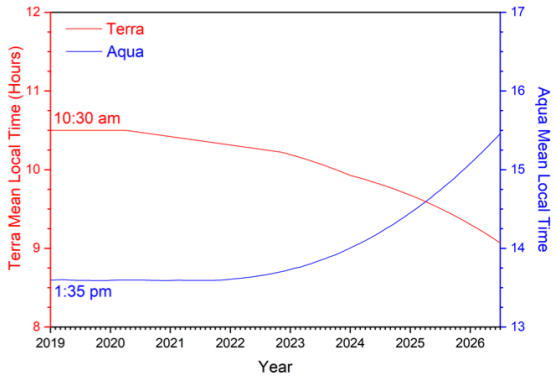

Figure 3-1. Terra and Aqua mean local equatorial crossing time (MLT) for January 2019 through July 2026.

- A full list of parameters on the CERES SSF1deg-Hour/Day/Month products is contained in their respective Data Product Catalogs (PDF):
  SSF1deg-Hour Data Product Catalog
  SSF1deg-Day Data Product Catalog
  SSF1deg-Month Data Product Catalog
- Users should be aware that some of the key inputs used to produce the SSF1deg changed at various times during the data record. Such changes, if large enough, may introduce spurious, unphysical jumps in the record. In the past, these changes were reflected in each CERES data product's version through a letter change (e.g., SRBAVG Edition2A, Edition2B, etc.). However, this proved cumbersome and confusing to many users. Therefore, for the SSF1deg product, letter changes will only reflect a reprocessing of the data record (e.g., due to a code bug). Major algorithm improvements will be noted as Editions. Changes to inputs are documented at the following web site: https://ceres.larc.nasa.gov/data/general-product-info/#ceres-input-data-sources. The web site provides a timeline of all input data source changes to date used to produce the SSF1deg Ed4A products. Users are advised to use this table as a reference in their analysis of SSF1deg products. See section 4.4 for examples of spurious jumps in the Ed3A record.
- Processing is performed on a nested grid (see Table 3-3). This grid uses 1° equal-angle regions between 45°N and 45°S and maintains area consistency at higher latitudes. The final products contain a complete 360x180 1° grid created by replication.

Table 3-3. CERES nested grid.

Latitude segment	# of zones in segment	Longitude extent (°)	# of regions/zone	# of regions in segment
Equator to 45°	90	1°	360	32400
45° to 70°	50	2°	180	9000
70° to 80°	20	4°	90	1800
80° to 89°	18	8°	45	810
89° to 90°	2	360°	1	2
Total	180	-	-	44012

- Zonal means are the average of all non-default regional values along a latitude band. Caution must be taken when using zonal means where there are many regional default values; examples are clear-sky SW and LW fluxes. No spatial interpolation is performed.
- The global mean is the geodetically area-weighted average of all 180 zonal means. The CERES geodetic weighting factors in look-up table format are located here: https://ceres.larc.nasa.gov/data/general-product-info/#geodetic-zone-weights-information. Where all the regional values are default, zonal means are interpolated between neighboring zones.
- Daily means are only available regionally. Daily zonal/global means are not available.

Fluxes

- In Ed3A, when the solar zenith angle was greater than 90°. twilight flux was added in SSF1deg to account for the atmospheric refraction of light (Kato and Loeb, 2003). In SSF1deg Ed4A, no twilight flux has been added to the daily and monthly SW flux means in order to maintain consistency between the Ed4A SSF1deg and SYN1deg products. For Edition 4, the SW twilight flux is only added in the EBAF product, since the EBAF product is a net flux balanced product. For the EBAF product, the twilight flux component is much smaller than the CERES instrument calibration adjustment.
- Despite recent improvements in satellite instrument calibration and the algorithms used to determine SW and LW outgoing TOA radiative fluxes, a sizeable imbalance persists in the average global net radiation at the TOA from CERES satellite observations. With the most recent CERES Edition4 instrument calibration improvements, the SSF1deg_Edition4A net imbalance is ~+5 W m^{-2} (see Table 5-2), which is much larger than the expected observed ocean heating rate of ~0.71 W m^{-2} (Johnson et al. 2016). If net balanced fluxes are required for the evaluation of climate models, for example, users are recommended to use the CERES EBAF Ed4A product. The EBAF dataset uses an objective constrainment algorithm to adjust SW and LW TOA fluxes within their ranges of uncertainty to remove the inconsistency between average global net TOA flux and heat storage in the Earth-atmosphere system.
- The CERES Edition 4 solar irradiance is from SORCE that is updated daily (SORCE Level 3 Total Solar Irradiance Version 15 available from: https://lasp.colorado.edu/data/tsis/tsi_data/tsis_tsi_L3_c24h_latest.txt. The SORCE total solar irradiance is ~1361 W m^{-2}. The SORCE observed solar irradiance will vary over the 11-year sunspot cycle with an amplitude of ~0.1%. (Note: The CERES EBAF-TOA Edition 4.2

solar irradiance is instead referenced to the TSI Community Composite model available here: https://spot.colorado.edu/~koppg/TSI/TSI_Composite-SIST.txt.)

- A processing glitch was discovered in the daily TSI file. The TSI daily fluxes during August 2019 and May through November 2020 (shown as the red values in Figure 3-2) were found to be scaled incorrectly resulting in a daily flux that was biased by ~ +0.8 W m^{-2}. The incorrect daily TSI fluxes (based on TSIS-1 TIM Version 3) were correctly scaled to the SORCE Version 15 reference and updated during February 2021. The SSF1deg TSI fluxes were impacted during August 2019 and May 2020 through November 2020. The resultant global averaged daily and monthly fluxes were found to be ~0.2 W m^{-2} too large out of a 20-year mean TSI flux of 339.88 W m^{-2}.

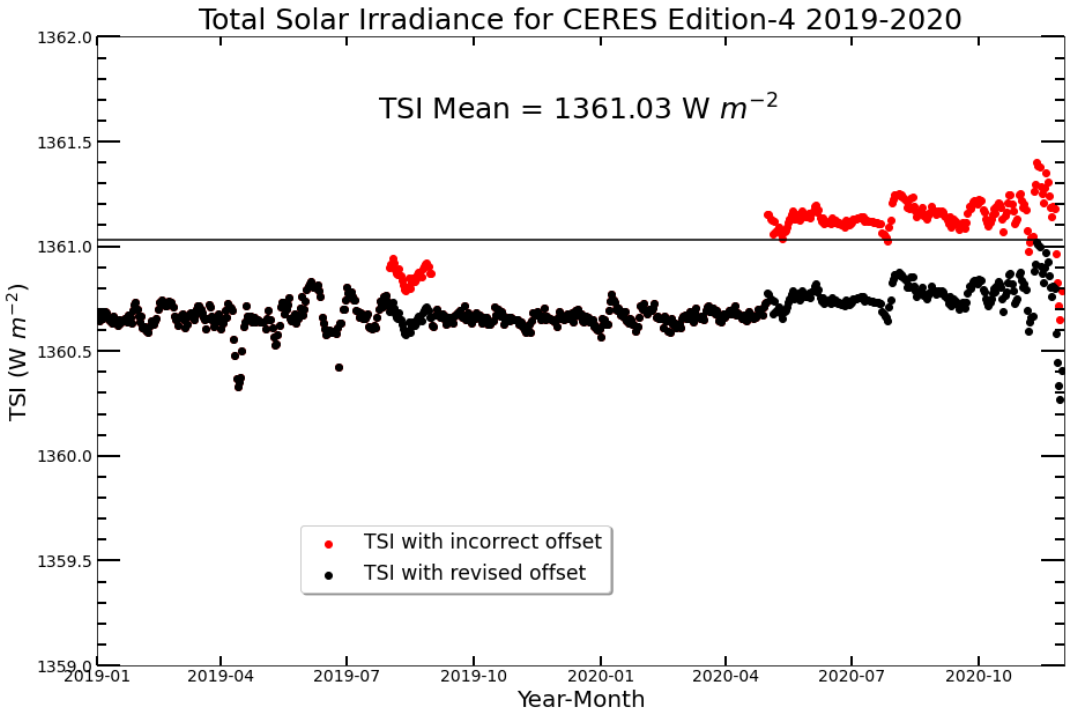

Figure 3-2. TSIS-1 TIM Version 3 at 1 AU incorrect scaling (red daily values) compared to the correct scaling (black daily values).

- Performing monthly deseasonalization or annual anomalies based on the 365-day calendar year (as opposed to 365.256 days for Earth to orbit the sun) may introduce unwanted variability in the CERES fluxes. Care must be taken when interpreting monthly anomalies. Please see the Appendix in section 10.0 for more information and examples.
- Geodetic, or oblate spheroid, weighting is used to derive the global flux mean from the zonal values. The geodetic Earth weights the tropics slightly more than the poles; the spherical Earth weights them equally (see Table 3-4). The spherical Earth assumption gives the well-known $S_o/4$ expression for mean solar irradiance, where S_o is the instantaneous solar irradiance at the TOA. When a more careful calculation is made by assuming the Earth is an oblate spheroid instead of a sphere, and when the annual cycles in the Earth's declination angle and the Earth-sun distance are taken into account, the division factor becomes 4.0034 instead

of 4. The following page provides the zonal geodetic weights used to determine global mean quantities:
https://ceres.larc.nasa.gov/data/general-product-info/#geodetic-zone-weights-information.

Table 3-4. The geodetic minus spherical earth annual global flux means.

Flux (W m^{-2})	SW reflected	LW emitted	Net	Solar incoming
All-sky	-0.18	+0.05	-0.16	-0.30
Clear-sky	-0.11	+0.06	+0.07	

- For clear-sky fluxes, if the region does not observe a single clear-sky (cloud fraction <0.1%) footprint for the month, the monthly mean is default. For some months, many regions do not contain clear-sky fluxes. Users wishing to have spatially complete regional clear-sky flux maps should utilize the EBAF product. In EBAF, the problem of gaps in clear-sky TOA flux maps is addressed by inferring clear-sky fluxes from both CERES and Moderate Resolution Imaging Spectrometer (MODIS) measurements to produce a new clear-sky TOA flux climatology that provides TOA fluxes in each 1°x1° region every month.
- The global mean is the geodetic area-weighted average of all 180 zonal means. Where all the regional values are default, zonal means are interpolated between neighboring zones. This interpolation occurs most frequently with SW flux near the polar night terminator. For SW flux the interpolation assumes constant albedo from the last available latitude. SW flux is calculated as the product of this albedo with analytically computed monthly mean solar insolation.
- Zonal and global parameters' means are not computed for the SSF1deg-Day Ed4A product. The geographical distribution and number of clear-sky regions are considered insufficient for a representative zonal and global mean. Fluctuations in the daily global mean are more likely to be attributed to spatial sampling and do not reflect the natural variation.
- The Terra and Aqua CERES instruments are placed on a common radiometric scale at the start of mission (March 2000 for Terra; July 2002 for Aqua). A detailed description of the radiometric scaling process for the Terra and Aqua instruments is provided here. The SNPP CERES instrument was radiometrically scaled to Aqua in 2014; details are provided here. The CERES instrument on NOAA-20 is also scaled to Aqua in May 2018. Please see the following link (slides 9-10) for further details.

Clouds

- Cloud properties are given for 4 static layers, low, mid-low, mid-high, and high based on effective cloud pressure and stratified between the surface, 700 hPa, 500 hPa, 300 hPa, and 50 hPa. The total cloud layer combines the 4 layers of cloud properties.
- The NOAA-20 VIIRS Ed2A cloud retrievals differ from NPP-VIIRS. The NOAA-20 VIIRS retrievals were designed to be similar to MODIS to improve continuity. The NOAA-20 VIIRS retrievals utilize CrIS based MODIS bands 27 (6.7 µm, WV) and 33 (13.3 µm, CO2) channel BT., whereas NPP does not. The non-polar cloud mask was modified to increase clouds over tropical ocean and reduce clouds over non-polar land regions. The polar cloud mask was tuned

to be more consistent the MODIS cloud mask. The MODIS-based 1.24μm and 3.7μm channel cloud reflectance models and parameterizations were used rather than those developed for VIIRS. A comparison shows that the NOAA-20 VIIRS global cloud fraction is 2.7% lower than Aqua-MODIS Ed4A. A summary of the cloud changes can be found here: https://ceres.larc.nasa.gov/documents/DQ_summaries/ssf_cloud_prop_noaa20_Ed1B.pdf.

- CERES SSF1deg provides both Day/Night (24-hour) and Day (solar zenith angle <90°) daily and monthly averaged cloud properties. The cloud optical depth, LWP, IWP, ice and liquid particle size retrieval algorithms differ between day and night. During the day both the MODIS visible and IR channels are used to compute these cloud properties, whereas at night the retrievals are limited to the IR channels.
- The SSF1deg Ed4A product provides two optical depth values. The traditional optical depth is spatially and temporally averaged in terms of log optical depth, since optical depth is exponentially proportional to radiance. The nontraditional optical depth, referred to as the linear optical depth, spatially and temporally averages the optical depth linearly. The combination of the linear and log optical depth is used to determine the distribution of the optical depth and should only be used for this purpose (Kato et al. 2005). When comparing the optical depth with other datasets, the log averaged optical depth should be used.
- The Ed4A MODIS cloud properties are based on upon Collection 5 through February 2016 and upon Collection 6.1 from March 2016 onwards. For Ed3A, the MODIS data were based on C4 until April 2006 and C5 thereafter. Also, Ed4A MODIS processing has mitigated the Terra-MODIS C5 calibration anomalies that occurred in July 2003 and in early 2009 that were especially apparent in the optical depth (see section 4.4.1).
- The Terra-MODIS water vapor (6.76-μm) channel performance has degraded after the Terra spacecraft anomaly event (February 18-28, 2016). Because this channel is mostly used to enhance cloud detection during polar night, cloud properties observed before and after the Terra spacecraft anomaly may be inconsistent over Antarctica and the Arctic Ocean during their months of polar night. The TOA OLR is not affected.
- In SSF1deg Ed4A, the cloud optical depth and particle size are based not only on the 3.7-μm channel, but also on the 1.2-μm and 2.1-μm channels. The 1.2-μm and 2.1-μm effective radiation is lower within the cloud than from the 3.7-μm channel; all three channels combined may offer a vertical profile of cloud microphysics. Cloud base temperature was also added in Ed4A.
- The SSF1deg Ed4A also provides a clear-sky detection quality indicator. The cloud mask clear-strong and clear-weak coverage parameters allow the user to determine the quality of the clear-sky observed. Large weak coverage indicates less certain clear-sky events.
- For SSF1deg Ed3A the liquid and ice cloud properties were temporally weighted by the total cloud fraction rather than by the corresponding liquid or ice fraction to determine the daily or monthly mean. This error was corrected in Ed4A.
- The CERES cloud properties are based on an update to the Minnis et al. (2011) cloud retrievals, which are contained in the CERES SSF Ed4A product. The SSF1deg-Hour/Day/Month products merely spatially and temporally average the existing CERES SSF footprint cloud properties. The quality of the MODIS cloud properties used in CERES are

summarized in the SSF Ed4A DQS. The CERES SSF1deg Ed4A product does not incorporate the NASA Goddard MODIS cloud properties.

Aerosols

- In the SSF1deg-Hour product, there is a discontinuity in the MODIS aerosols beginning in March 2017 attributed to the change from MODIS Collection 5 to Collection 6. Please do not use these aerosols for trend studies.
- In the SSF1deg-Day/Month products, MODIS Collection 6.1 aerosols are used throughout if you are obtaining these from the CERES Ordering Tool.

Auxiliary Parameters

- The SSF1deg Ed4 has added the following GEOS atmosphere parameters: skin temperature, surface pressure, the surface minus 750 mb temperature and 750 mb potential temperature minus surface temperature differences, inversion strength, and wind speed.
- SSF1deg Ed4A products are based upon consistent meteorological assimilated data (GEOS 5.4.1) throughout the record. The Edition 3 was processed with GEOS 4.0 until December 2007 and processed with GEOS 5.2 beginning in January 2008. This caused a discontinuity when comparing atmospheric parameters over the CERES record (see section 4.4.2).

4.0 Version History

4.1 Changes Between the Initial and Revised Versions of SSF1deg Ed4A

After the initial release of SSF1deg-Day/Month Ed4A, several issues were found; a revised version of the SSF1deg-Day/Month Ed4A was released (see Cautions and Helpful Hints). These issues do not affect the SSF1deg-Hour Ed4A product.

The Edition 4 snow and ice directional models (diurnal albedo models as a function of solar zenith angle) were not implemented in the initial SSF1deg Ed4A version, which incorrectly used the TRMM theoretical snow directional models. All previous Editions including SSF1deg Ed3A also used the TRMM theoretical snow and ice directional models. The TRMM precessionary satellite orbit was confined to the tropical latitudes and had insufficient snow observations to adequately build empirical snow and ice directional models and thus relied on theoretical models. The Ed4A snow and ice directional models are derived from Terra and Aqua SW fluxes using the same scene conditions that the Ed4A angular directional models utilize. The Ed4A snow and ice directional models are considered more accurate. The monthly regional TRMM minus Ed4A snow and ice directional model biases are shown in Figure 4-1. Although the biases can be either positive or negative depending on whether the scene is over permanent snow, sea ice or fresh snow over land, the Ed4A directional models generally have increased the daily flux over snow regions. The monthly global all-sky SW bias impact varies from 0.15 to 0.45 W m^{-2} as shown in Figure 4-2 over both the Terra and Aqua records.

There has been a bug fix in the temporal interpolation process for albedos, which are used to obtain SW fluxes. The wave pattern seen in Figure 4-1 for the all-sky SW fluxes has been eliminated in the revised version of SSF1deg Ed4A.

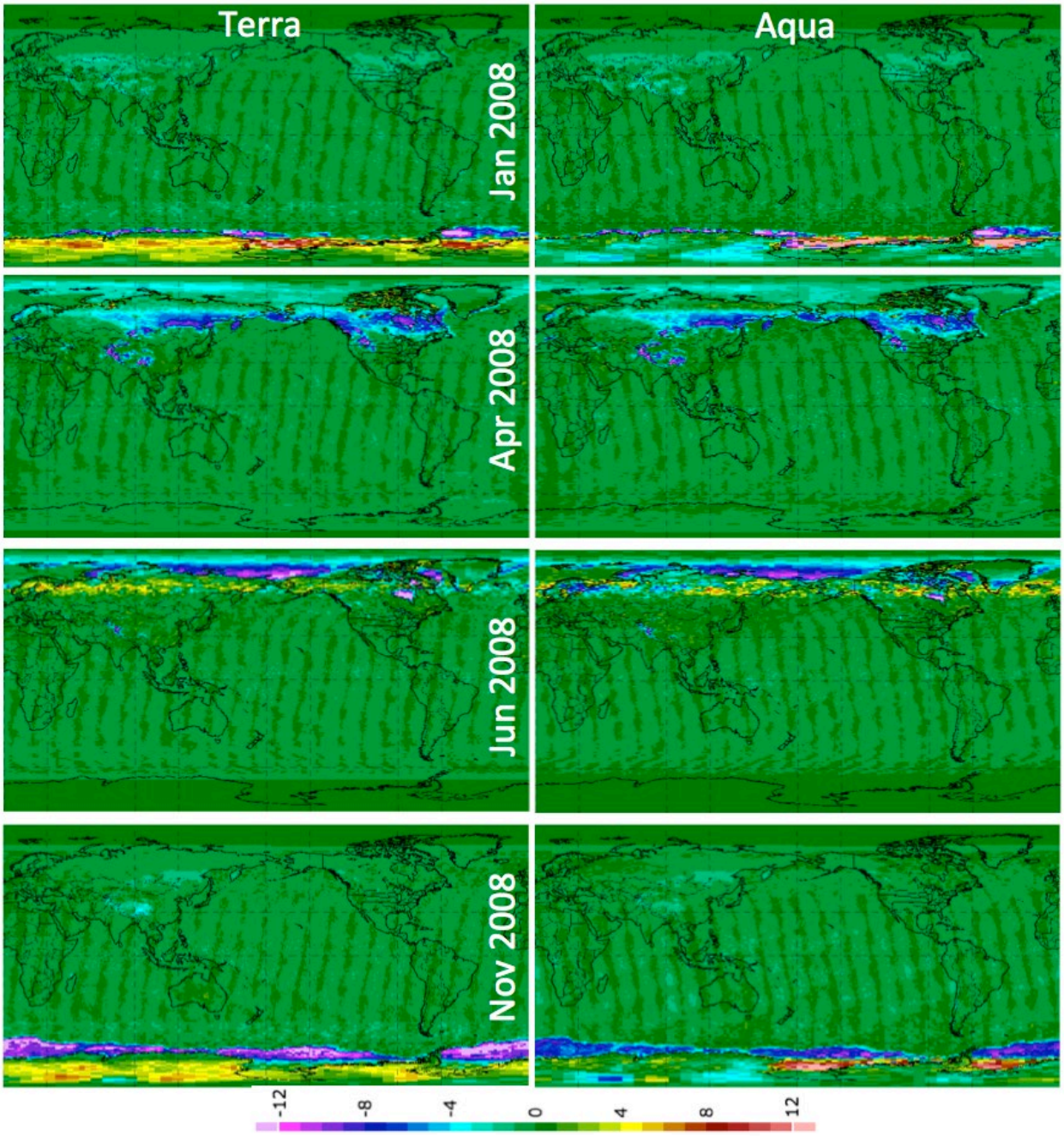

Figure 4-1. The monthly regional all-sky SW initial minus revised SSF1deg Ed4A bias for (left panel) Terra and (right panel) Aqua for Jan. 2008, Apr. 2008, June 2008, and Nov. 2008. The revised Ed4A (empirical Ed4A snow and ice directional models) is considered more accurate than the initial version (theoretical TRMM directional models). The bias scale is shown between the June 2008 and Nov. 2008 plots; units are W m^{-2}.

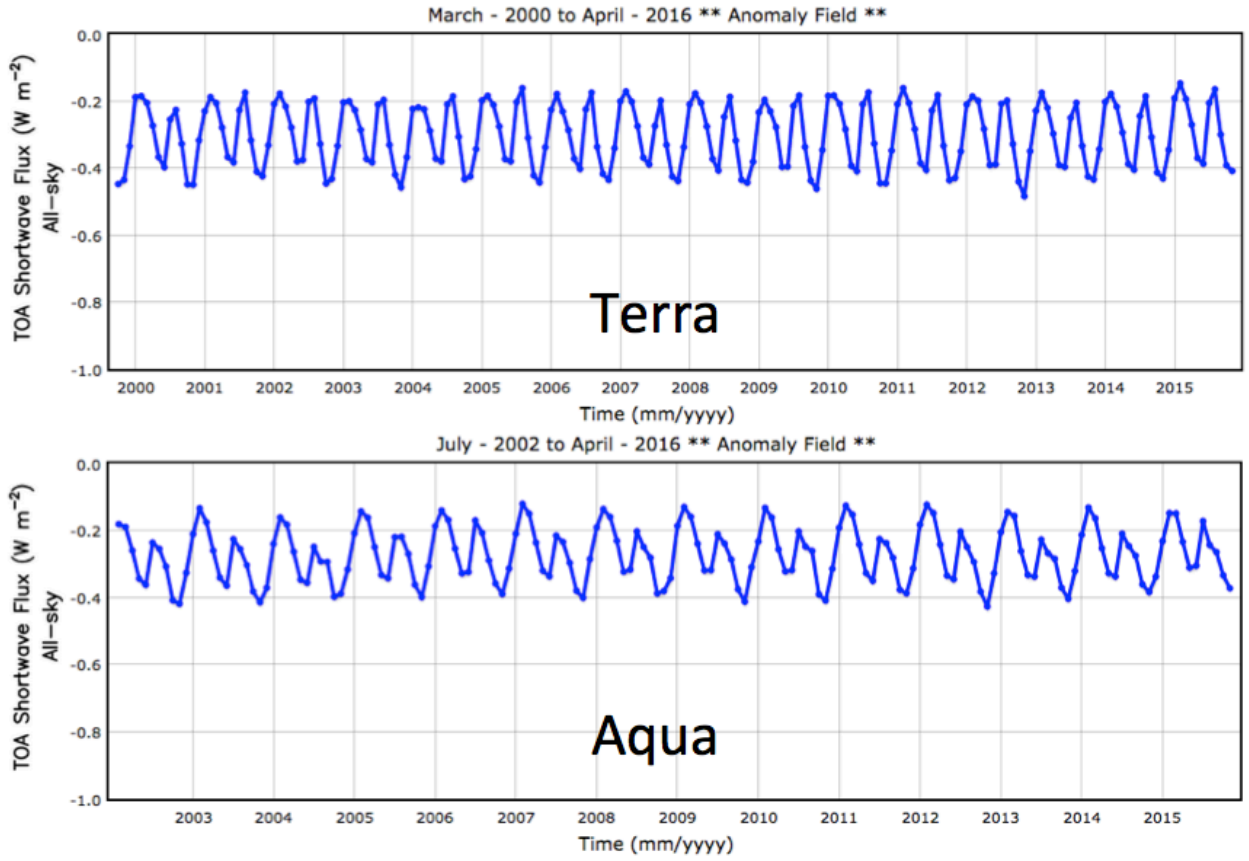

Figure 4-2. The monthly global all-sky SW initial minus revised SSF1deg Ed4A bias for (top) Terra and (bottom) Aqua over their respective records. The revised Ed4A (empirical Ed4A snow and ice directional models) is considered more accurate than the initial version (theoretical TRMM directional models).

On rare occasions, a clear-sky ocean SW measurement is incorrectly converted into a daily averaged flux due to a coding error. The impact can be seen in Figure 4-3, which displays the initial minus revised SSF1deg Ed4A monthly regional clear-sky SW flux. The ocean to the east of Australia shows a positive bias (~5 W m^{-2}) for Terra during June 2008. Underestimation of the SW clear-sky flux (~-4 W m^{-2}) is seen to the east of Hawaii and to the west of Canada for both Terra and Aqua. Note that the clear-sky SW flux is also impacted in snow/ice regions due to the use of the incorrect TRMM theoretical snow directional models, explained in the paragraph above. This error did not impact the SSF1deg Ed3A.

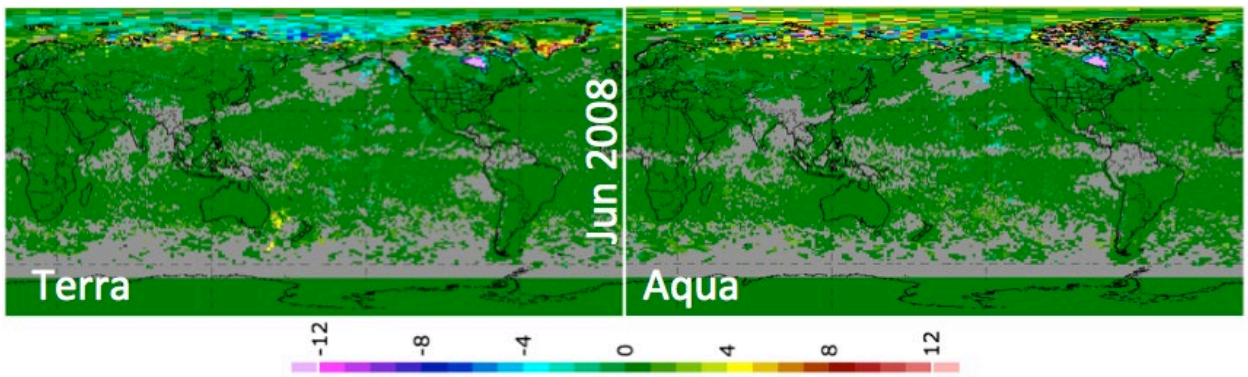

Figure 4-3. The monthly regional clear-sky SW initial minus revised SSF1deg Ed4A bias for June 2008 for both Terra (left) and Aqua (right). Units are W m^{-2}.

The CERES snow and ice fraction is a combination of 1) the permanent snow and ice fraction from IGBP, 2) the National Snow and Ice Data Center (NSIDC) daily snow and ice, and 3) the CERES cloud mask snow/ice history map for water locations within 50 km from any coastline. The last component was implemented in Ed4A to account for the sea ice not seen by the microwave data. In the initial SSF1deg Ed4A dataset, the last component was added to the snow/ice coverage parameter but was not subtracted from the ocean coverage parameter. Figure 4-4 shows the impact of this error in the ocean coverage, where the initial SSF1deg Ed4A ocean coverage is overestimated when compared to the revised version.

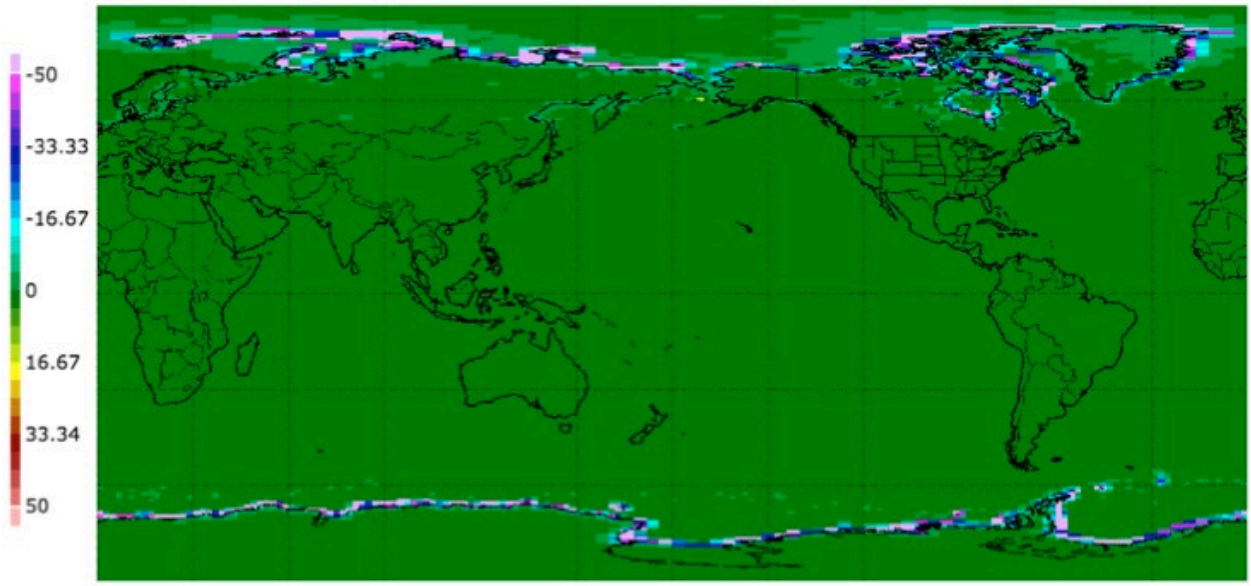

Figure 4-4. The monthly regional ocean coverage initial minus revised SSF1deg Ed4A bias for June 2008 for Terra. Units are percent.

In the initial SSF1deg Ed4A dataset, LWP and IWP were not computed from optical depth and particle size and were simply temporally interpolated. Therefore, LWP and IWP are inconsistent with the optical depth and particle size. In the revised version, LWP and IWP are consistent with the optical depth and particle size.

4.2 Algorithm Changes Between SSF1deg Ed3A and SSF1deg Ed4A

This section highlights the CERES algorithm changes and improvements made in the Ed4A products. In Ed4A, the CERES instrument calibration and temporal trending of the spectral response functions are updated. The MODIS cloud properties are updated with emphases on polar cloud properties and consistency between Terra and Aqua MODIS retrievals (Minnis et al. 2011, SSF Edition4A Data Quality Summary). The cloud fraction now agrees more with CALIPSO. The ADMs are updated and incorporate the Ed4A MODIS cloud properties (Su et al. 2015a, Su et al. 2015b, SSF Edition4A Data Quality Summary). The spatial gridding of the CERES footprint fluxes and temporal interpolation algorithms have not changed for Ed4A. The SW and LW diurnal models continue to be based on the constant meteorology at the time of the CERES and MODIS observation as described in Young et al. (1998).

4.3 Input Changes Between SSF1deg Ed3A and SSF1deg Ed4A

This section highlights the major input changes between the SSF1deg Ed3A and Ed4A products. The CERES project strives to process the entire data record using consistent version input sources as well as processing the CERES editions with the same algorithms. Any change in the input version or processing algorithm may introduce artifacts in the record and should not be interpreted as natural variability. This requirement is sometimes difficult to achieve, since input versions may be discontinued.

A complete list of input version changes are listed on the following website: https://ceres.larc.nasa.gov/data/general-product-info/#ceres-input-data-sources. The two most significant input changes are in the versions of the MODIS and GEOS products (Table 4-1).

Table 4-1. The MODIS and GEOS versions used in SSF1deg Ed3A and Ed4A.

	Ed3A	Ed4A
MODIS	Collection 4 from Mar 2000 Collection 5 from Apr 2006	Collection 5 from Mar 2000 Collection 6 from Mar 2017
GEOS	GEOS-4 from Mar 2000 GEOS-5.2 from Jan 2008 GEOS-5.4.1 from March 2016	GEOS-5.4.1 from Mar 2000

4.4 Ed4A Input Improvements over Ed3A

In this section, the major Ed3A input trend anomalies are discussed along with their Ed4A improvements. Comparison plots show the impacts.

4.4.1 Terra Cloud Optical Depth

The Terra-MODIS instrument band 1 (0.65-µm) experienced two calibration anomalies over the CERES record. Both MODIS instruments rely on lunar looks and the solar diffuser for on-orbit stability. The first anomaly occurred on July 2, 2003, when the solar diffuser door on the Terra-MODIS malfunctioned and was left in the open position. This darkened the Terra-MODIS optics by 1% (Minnis et al. 2008) and was unaccounted for in the Collection 5 dataset. The second anomaly occurred in early 2009, when the solar diffuser degradations were observed to be 1.5%

and 0.3% for Terra-MODIS and Aqua-MODIS, respectively, but these were not corrected in the Collection 5 calibration (Wu et al. 2013). The CERES cloud retrieval code mitigated both calibration anomalies by adjusting the Terra-MODIS radiances. (See https://asdc.larc.nasa.gov/documents/ceres/quality_summaries/ssf_cloud_prop_terra-aqua_Ed4A.pdf.) These two Terra-MODIS calibration anomalies are easily identified in the Ed3A daytime optical depth record during 2003 and 2009 in Figure 4-5. By explicitly accounting for these calibration anomalies in Ed4A, the cloud optical depths are now consistent over the record.

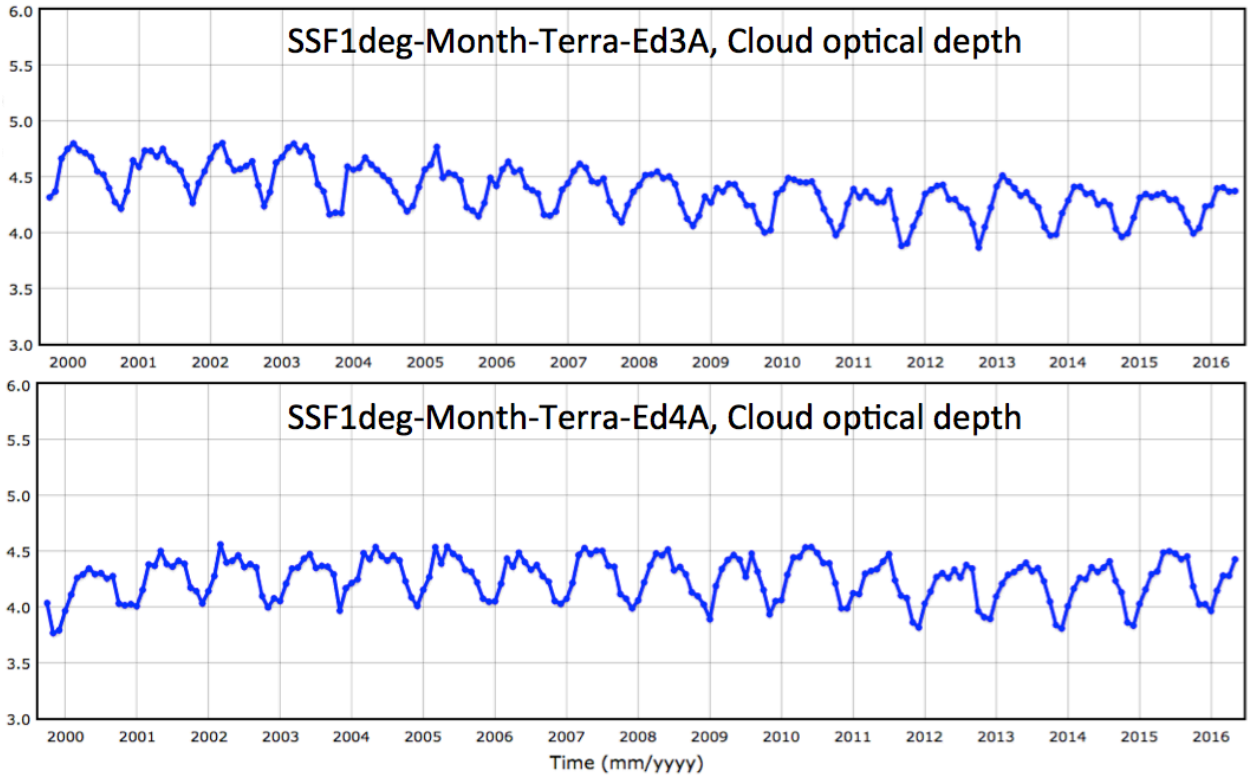

Figure 4-5. Comparison of the SSF1deg Terra-MODIS global monthly mean optical depth (daytime only) between Ed4A and Ed3A. Note the Terra-MODIS C5 calibration anomalies during 2003 and 2009 for Ed3A are mitigated by Ed4A processing.

4.4.2 GEOS Versions

All CERES Edition 4A products are based upon consistent meteorological assimilated data (GEOS-5.4.1) throughout the record, whereas in Ed3A, GEOS-4 was replaced with GEOS-5.2 during January 2008 (see Table 4-1). This impacted the clear-sky LW flux during 2008 in Ed3A (Figure 4-6). The GEOS precipitable water (PW) showed a discontinuity in the Ed3A record due to the GEOS version transition (Figure 4-7). Consistent use of the GEOS-5.4.1 atmosphere in Ed4A removes the discontinuity in both the clear-sky LW and PW global monthly means.

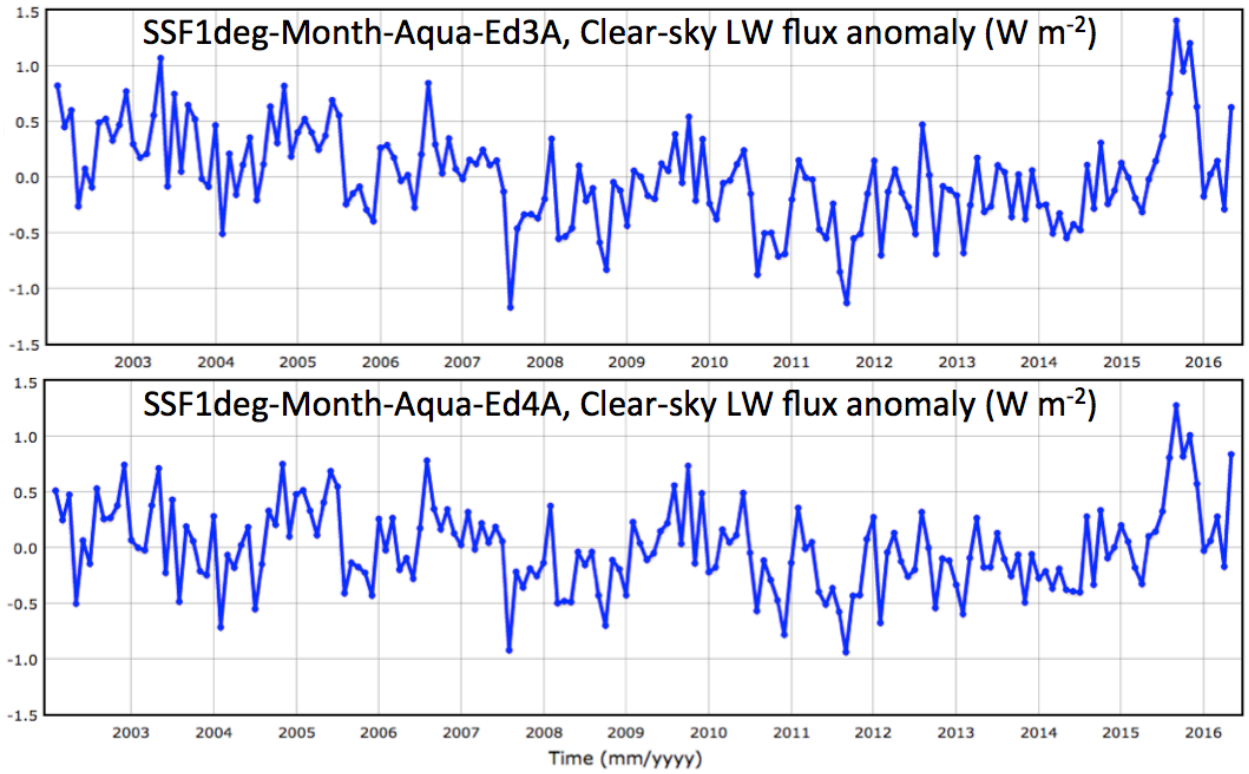

Figure 4-6. Comparison of the SSF1deg Aqua global monthly mean clear-sky LW TOA flux anomalies between Ed4A and Ed3A. Note the Ed3A discontinuity during January 2008 coincides with the transition between GEOS-4.0 and GEOS-5.2. GEOS-5.4.1 has been used over the entire Ed4A record.

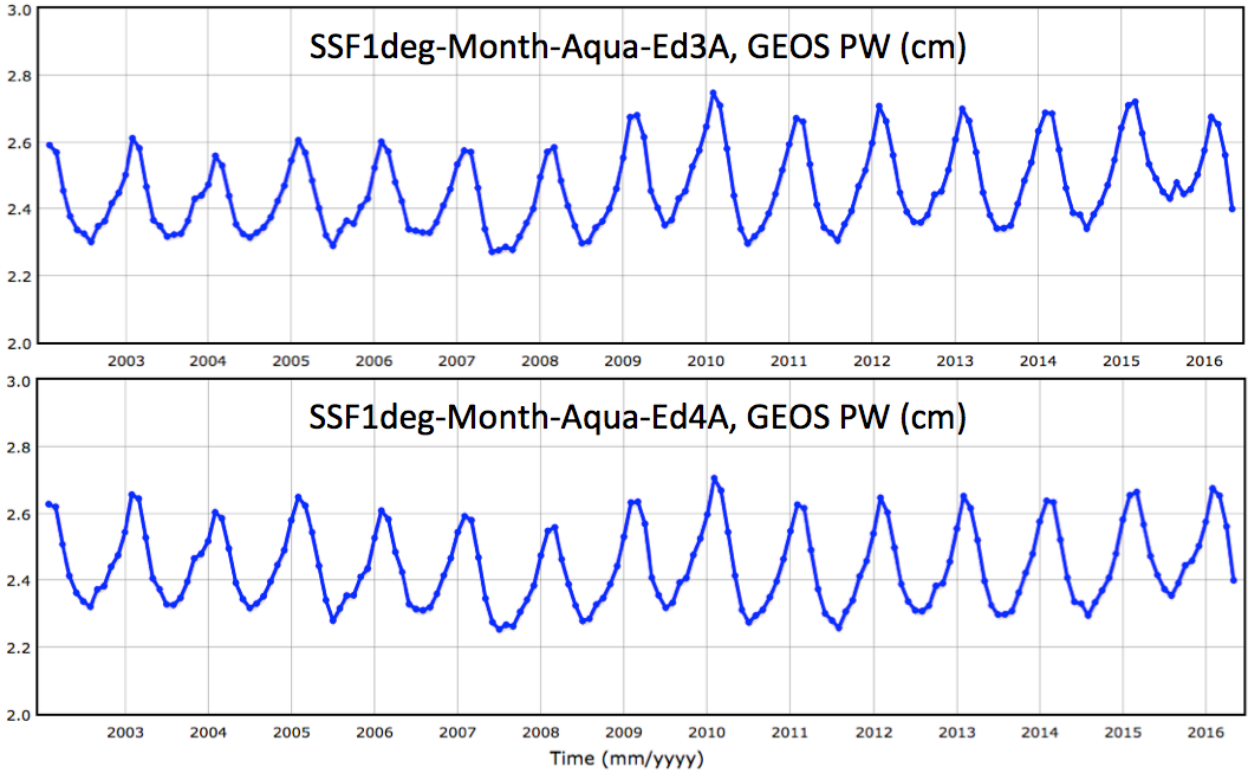

Figure 4-7. Same as Figure 4-6 except for precipitable water (PW).

4.4.3 MODIS Land Aerosol Optical Depth

For Ed3A, the MODIS data were based on Collection 4 until April 2006 and Collection 5 thereafter. The land aerosol optical depths, which are based on the NASA-GSFC MODIS MOD04_L2 retrievals, show a discontinuity in the Ed3A dataset during the C4 to C5 transition (Figure 4-8). Due to the consistent use of MODIS Collection 5 during the Ed4A processing, the aerosol optical depths now show no apparent trends.

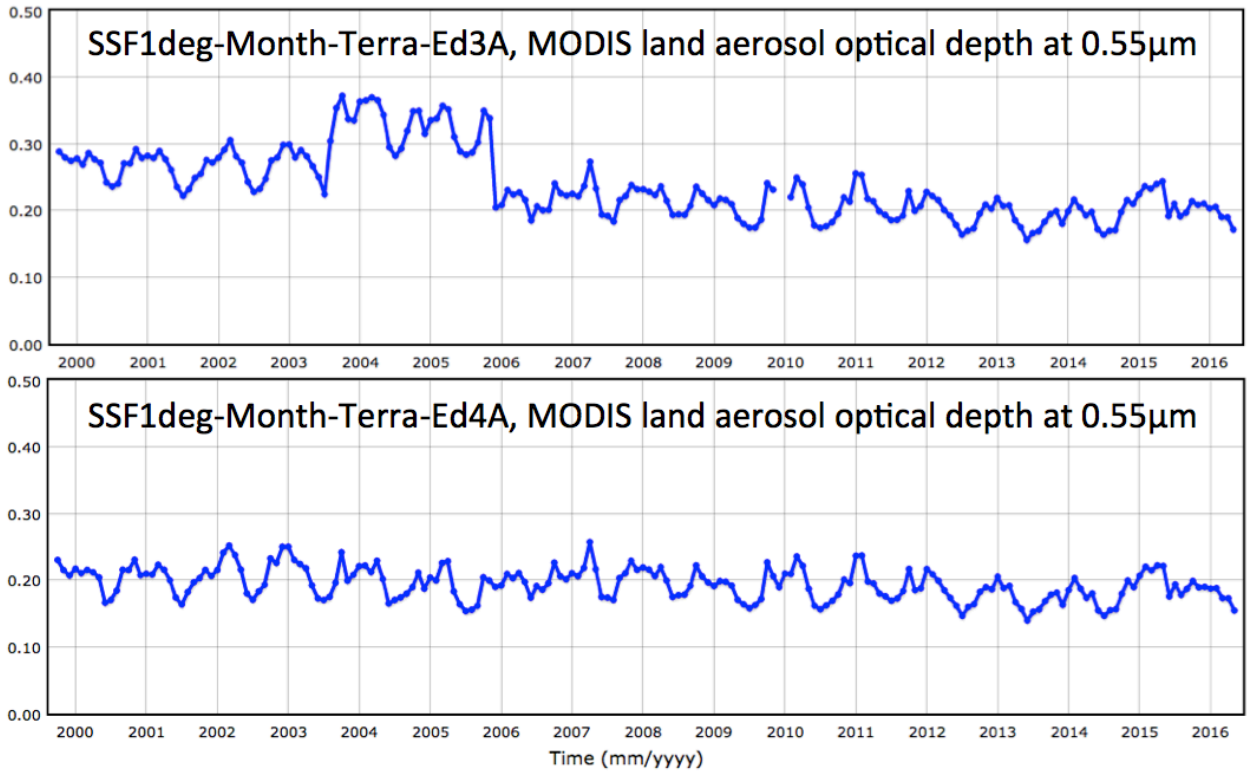

Figure 4-8. Comparison of the Terra-MODIS global monthly mean land aerosol optical depth at 0.55 µm between Ed4A and Ed3A. Note the Ed3A discontinuity during April 2006 coincides with the transition between MODIS Collections 4 and 5.

4.5 Ed4A Input Trend Anomalies

The major known Ed4A input trend anomalies are highlighted. These are not expected to be corrected until Edition 5.

4.5.1 CERES Terra-MODIS Cloud Phase

The Terra-MODIS SSF1deg-month Ed4A cloud phase seems to trend towards increasing ice clouds after 2010, especially for nighttime retrievals (Figure 4-9). The Ed3A phase did not exhibit a trend. Also, the Aqua-MODIS SSF1deg Ed3A and Ed4A cloud phase do not seem to trend.

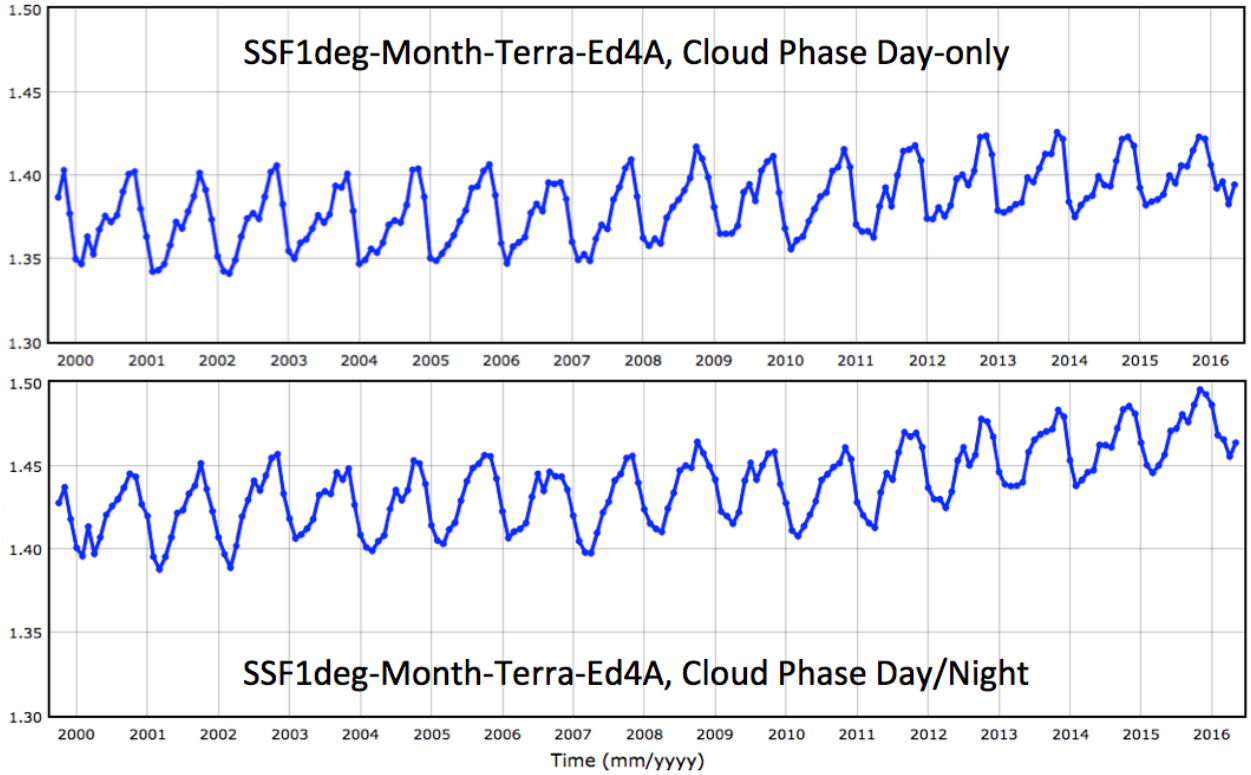

Figure 4-9. The Terra SSF1deg Ed4A global monthly mean cloud phase for (top) day-only and (bottom) day and night. Cloud phase of 1 indicates liquid cloud and 2 indicates ice. The cloud phase did not have a trend in Ed3A.

4.5.2 CERES Terra-MODIS 1.2-µm Channel Cloud Properties

Traditionally, optical depth, ice particle size, and liquid particle size are based on the 3.7-µm channel and are provided by both the Ed3A and Ed4A SSF1deg datasets. For SSF1deg-Ed4A, two additional cloud optical depths and particle sizes are provided based on the 1.2-µm, and 2.1-µm MODIS channels. Users should be aware that the Terra-MODIS 1.2-µm channel has a calibration anomaly in 2002 that causes a discontinuity for the cloud properties based on that channel (Figure 4-10). However, no 1.2-µm cloud property anomalies are observed within the SSF1deg-Ed4A Aqua product.

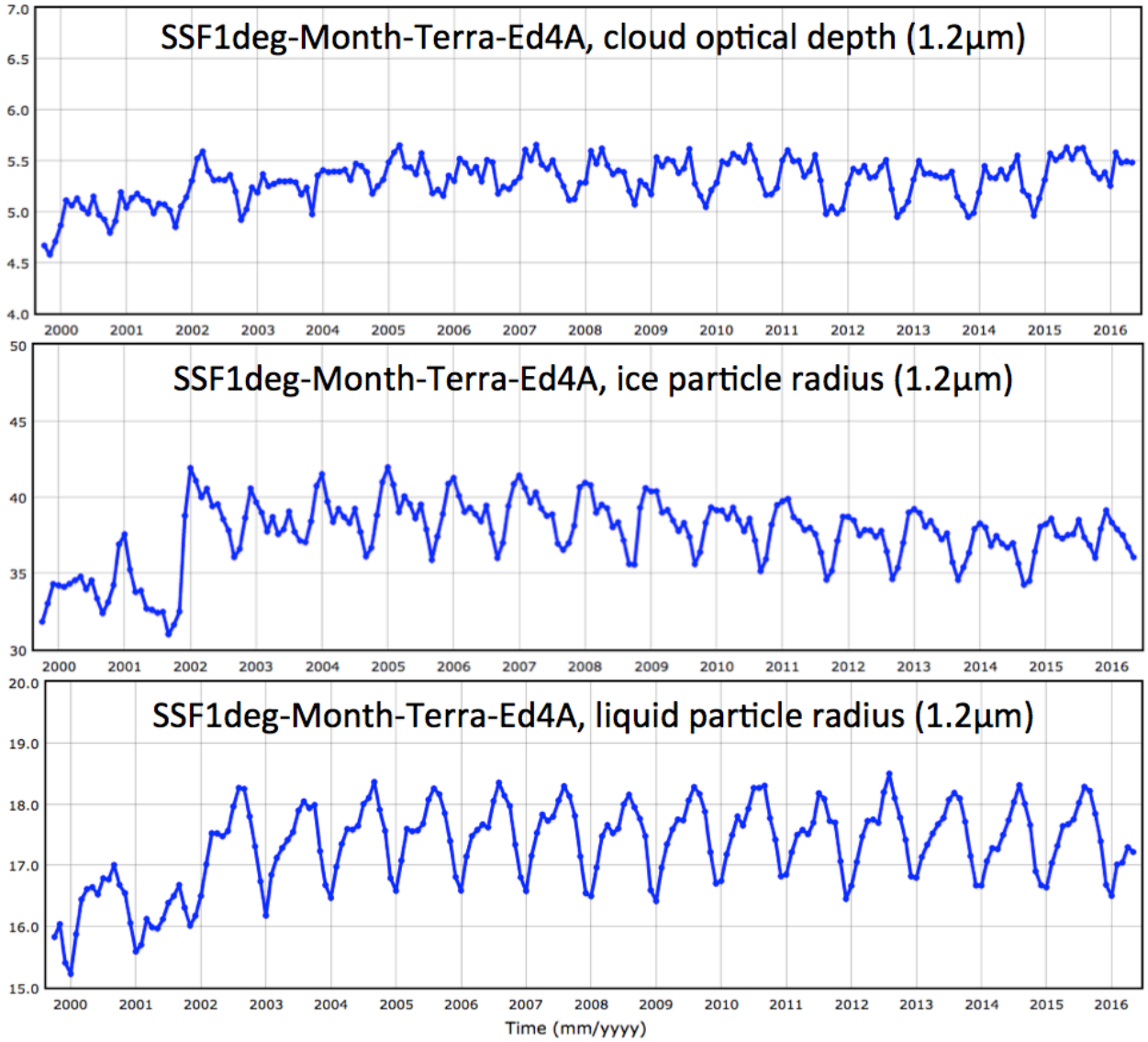

Figure 4-10. The Terra SSF1deg Ed4A global monthly mean cloud optical depth (top), ice particle size (middle), and liquid particle size (bottom) for daytime only based on the Terra-MODIS 1.2-µm channel. Units of particle size are µm.

5.0 Accuracy and Validation

5.1 SSF1deg Ed4A Uncertainties

The monthly 1°x1° regional all-sky SW flux uncertainty is due to: 1) CERES instrument calibration uncertainty of 1 W m^{-2} (1σ), 2) the radiance-to-flux conversion error of 1 W m^{-2} (1σ) (Su et al. 2015b), and 3) the diurnal correction (based on constant meteorology) uncertainty of 6 W m^{-2} (Doelling et al. 2013). The diurnal correction uncertainty value is based on comparisons with Geostationary Earth Radiation Budget (GERB) observed broadband SW fluxes. The diurnal correction may be overestimated, since the GERB geostationary domain has a disproportionate number of strong diurnal cycle regions as compared with the globe. The combined monthly regional all-sky SW flux uncertainty is 6.2 W m^{-2}. The daily regional all-sky SW diurnal uncertainty is 20 W m^{-2} (Doelling et al. 2013).

The monthly 1°x1° regional all-sky LW flux uncertainty is due to: 1) CERES instrument calibration of 1.8 W m^{-2} (1σ), 2) the radiance to flux conversion 0.75 W m^{-2} (1σ) (Su et al. 2015b), and 3) the diurnal correction of 6 W m^{-2} (Doelling et al. 2016). The diurnal correction uncertainty value is based on comparisons with GERB observed broadband LW fluxes. Again, the diurnal model uncertainty may be overestimated. The combined regional all-sky LW flux uncertainty is 2.4 W m^{-2}. The daily regional all-sky LW diurnal uncertainty is 8 W m^{-2} (Doelling et al. 2016).

The cloud property uncertainties may be obtained from the SSF Ed4A Data Quality Summary: https://asdc.larc.nasa.gov/documents/ceres/quality_summaries/CER_SSF_Terra-Aqua_Edition4A.pdf.

5.2 SSF1deg Ed4A and Ed3A Cloud and Flux Comparisons

This section highlights the CERES SSF1deg Ed4A and Ed3A TOA SW and LW differences. The CERES instrument calibration and CERES instrument spectral response function corrections, MODIS cloud properties, and ADMs were improved in Ed4A. These improvements have caused some regional SW and LW flux Ed4A and Ed3A differences, which are highlighted in this section. The constant meteorology SW and LW flux temporal interpolations needed to compute daily mean fluxes from the instantaneous observed CERES fluxes were not changed in Ed4A. There were also changes to the cloud properties, which had an impact on the clear-sky fluxes. The cloud properties will be discussed first.

The Edition 4 MODIS cloud mask provides the greatest cloud retrieval improvement. The new cloud mask substantially improves detection of thin cirrus and low cloud, provides a better discrimination between cloud and dust, and substantially improves cloud detection in polar regions. The cloud mask improvements include the use of additional MODIS channels and threshold tests (MODIS 1.38-µm threshold test, T3.7-T11 and T11-T12 difference tests, 2.1- to 0.6-µm ratio test, 1.24- to 0.65-µm ratio test, and new VIS threshold tests) derived with the benefit of years of CALIPSO data for guidance.

The Ed4A MODIS retrieved cloud fraction has increased from Ed3A to better match the CALIPSO-detected clouds. Figure 5-1 displays the Ed4A minus Ed3A cloud fraction for January and July 2010 for both Terra and Aqua. Over the tropics, the Ed4A MODIS cloud mask detects

more high thin clouds near the ITCZ. Also, more sub-pixel low clouds are identified as illustrated by the West Pacific Ocean domain north of the ITCZ for Aqua July 2010 and for regions where the cloud fraction is less than 50%. An increase of up to 20% is shown in the difference plot. The polar cloud mask was improved to detect clouds over broken sea ice near the poles (see Figure 5-1 Aqua Jan 2010 over the North Pole and in July 2010 near Antarctica). The Ed3A land cloud algorithm employed two retrieval domains divided at 60°N during July (as seen in both Terra and Aqua plots). The Ed4A cloud code removes this retrieval discontinuity. Figure 5-2 shows the Ed4A minus Ed3A day/night total cloud fraction over the Terra and Aqua records with a consistent 6% increase in cloud fraction for both satellites.

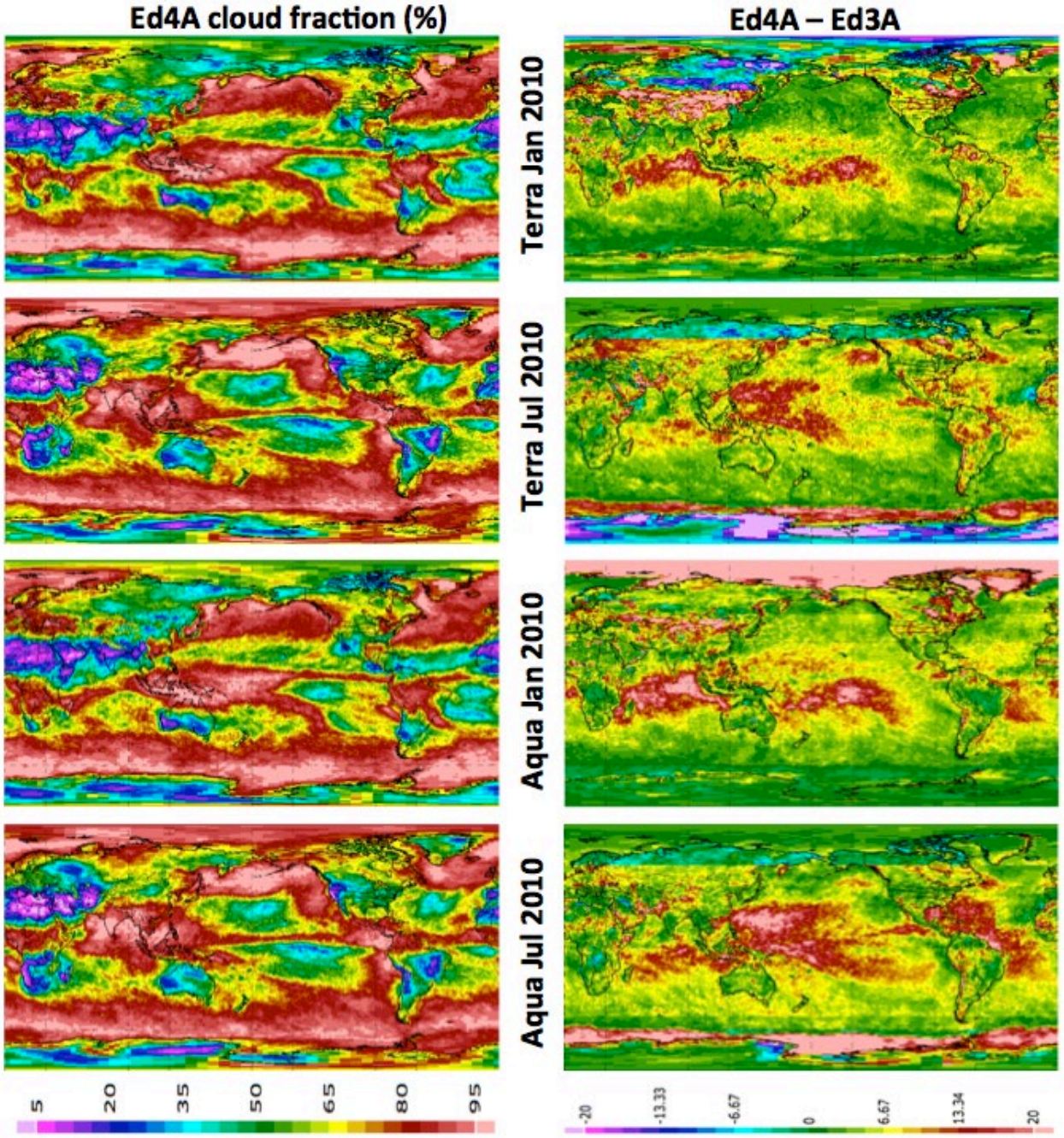

Figure 5-1. (left panels) The regional monthly mean total cloud fraction (%) for SSF1deg Ed4A

and (right panels) for SSF1deg Ed4A minus Ed3A for (top row) Terra Jan. 2010, (2nd row) Terra July 2010, (3rd row) Aqua Jan. 2010, and (bottom row) Aqua July 2010.

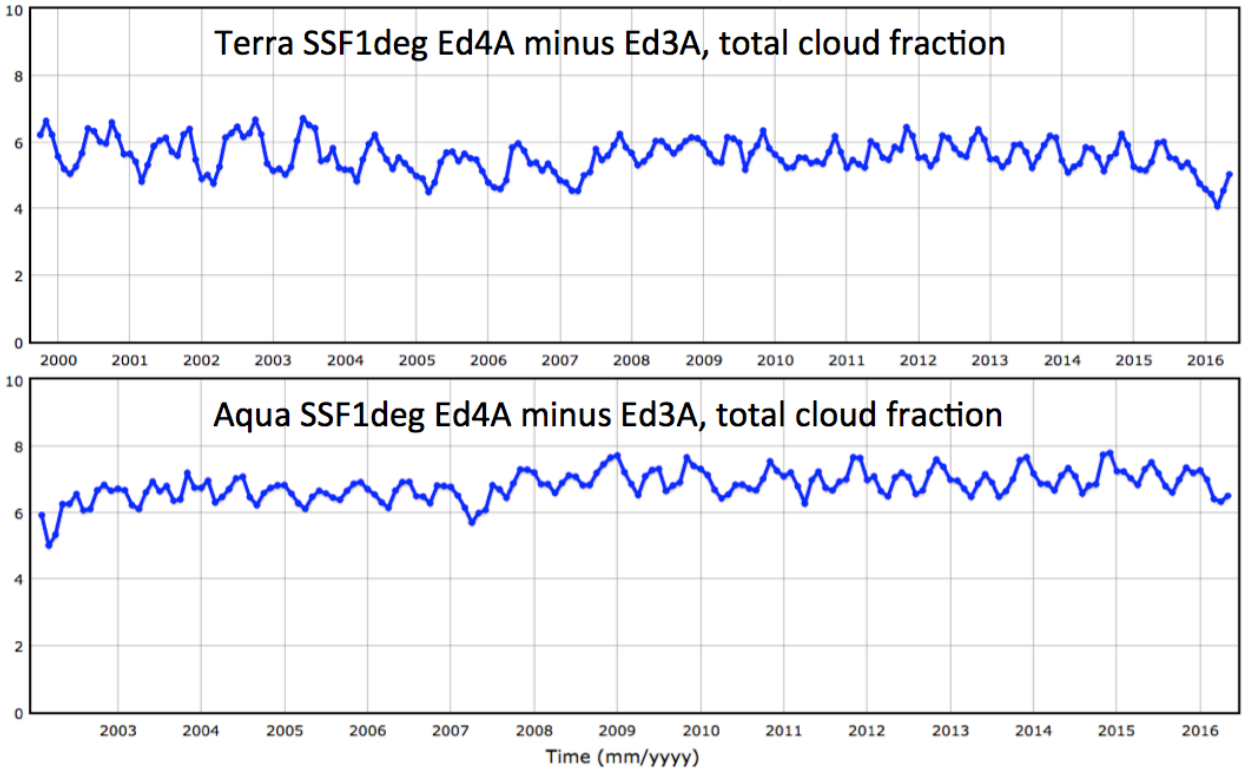

Figure 5-2. The SSF1deg Ed4A minus Ed3A global monthly mean day/night total cloud fraction (%) for (top) Terra and (bottom) Aqua.

Table 5-1 displays the 2003-2015 mean global cloud properties for Ed3A and Ed4A for both satellites for day-only and for day/night (24 hours). In Ed4A, the cloud fraction increases by ~3% for day-only and by ~6% for day/night. This suggests that the night-only Ed4A cloud fraction increased more at night than the day-only cloud fraction compared to Ed3A. Very small Ed4A and Ed3A changes in the daytime optical depth and nighttime IR emissivity indicate that the Ed4A cloud mask detected more thin or sub-pixel clouds, that is, clouds with very small optical depth. The cloud phase changes indicate that more liquid sub-pixel low clouds are detected when compared with high thin ice clouds. The cloud effective temperature is slightly smaller in Ed4A due to the increased detection of high thin clouds. An increase in high clouds has a greater impact on the global mean cloud temperature, since the high clouds have a much greater temperature contrast with the respect to the surface than do low clouds.

Table 5-1. The 2003-2015 13-year global mean cloud amount (%), cloud optical depth, cloud phase (1.0=liquid, 2=ice), cloud effective temperature (K), and cloud IR emissivity for daytime (SZA<90°) and day/night (24-hour) MODIS cloud properties for CERES Terra and Aqua SSF1deg Ed3A and Ed4A data products.

Dataset	Daytime Cloud					Day/Night Cloud			
SSF1deg	Amount (%)	Optical Depth	Phase	Temp (K)	IR Emiss	Amount (%)	Phase	Temp (K)	IR Emiss
Terra Ed3A	62.1	4.34	1.42	261.4	0.83	61.5	1.50	256.3	0.80
Terra Ed4A	65.8	4.25	1.38	260.3	0.83	67.1	1.44	255.8	0.76
Aqua Ed3A	63.2	4.07	1.48	260.2	0.83	61.3	1.51	256.6	0.76
Aqua Ed4A	66.6	4.10	1.39	259.6	0.82	68.1	1.43	256.1	0.76

Figure 5-3 and Figure 5-4 display the SSF1deg Ed4A minus Ed3A SW and LW fluxes and associated trend differences for Terra and Aqua, respectively. Most of the SW Ed4A minus Ed3A flux differences are due to the improvements in the ADMs; these improvements should be similar for Terra and Aqua. Most notably, the Ed4A SW flux slightly decreases over the Antarctic sea ice domain and increases over convective land regions compared to Ed3A for both Terra and Aqua platforms. The Terra and Aqua ADMs are constructed separately so that the MODIS cloud property differences between Terra and Aqua do not impact the derived fluxes. Also, the albedo temporal interpolation fix in Ed4A (section 4.1) has removed the wave pattern seen in the SW flux difference. The Ed4A minus Ed3A LW fluxes show a slight decrease over land and an increase over oceans with low cloud fractions. This difference is greater for Aqua than Terra.

Figure 5-3 displays the Ed4A minus Ed3A SW and LW all-sky trend difference for Terra. The SW trend difference is slightly negative and is related to the negative optical depth trend for Terra (see Figure 4-5). The SW radiance to flux conversion is based on optical depth, cloud fraction, and cloud phase. If the optical depth changes over time, the ADM scene will also change over time causing a residual trend in the SW flux (see the EBAF Ed4.0 Data Quality Summary). There are also small negative trends in the Ed4A minus Ed3A Aqua SW and LW (Figure 5-4) mainly due to positive differences in each of them during the first two years (Figure 5-5). The Aqua SW trend difference is mostly negative over ocean (Figure 5-4), and the LW trend difference is mostly negative over land. When comparing the SSF1deg Ed3A LW global monthly means with EBAF Ed4.0, a small trend is manifested (EBAF combines Terra and Aqua observations), whereas the Ed4A did not indicate a trend (not shown). This suggests that the SSF1deg Ed4A product removes the SW and LW residual trends that are present in the Ed3A SSF1deg product.

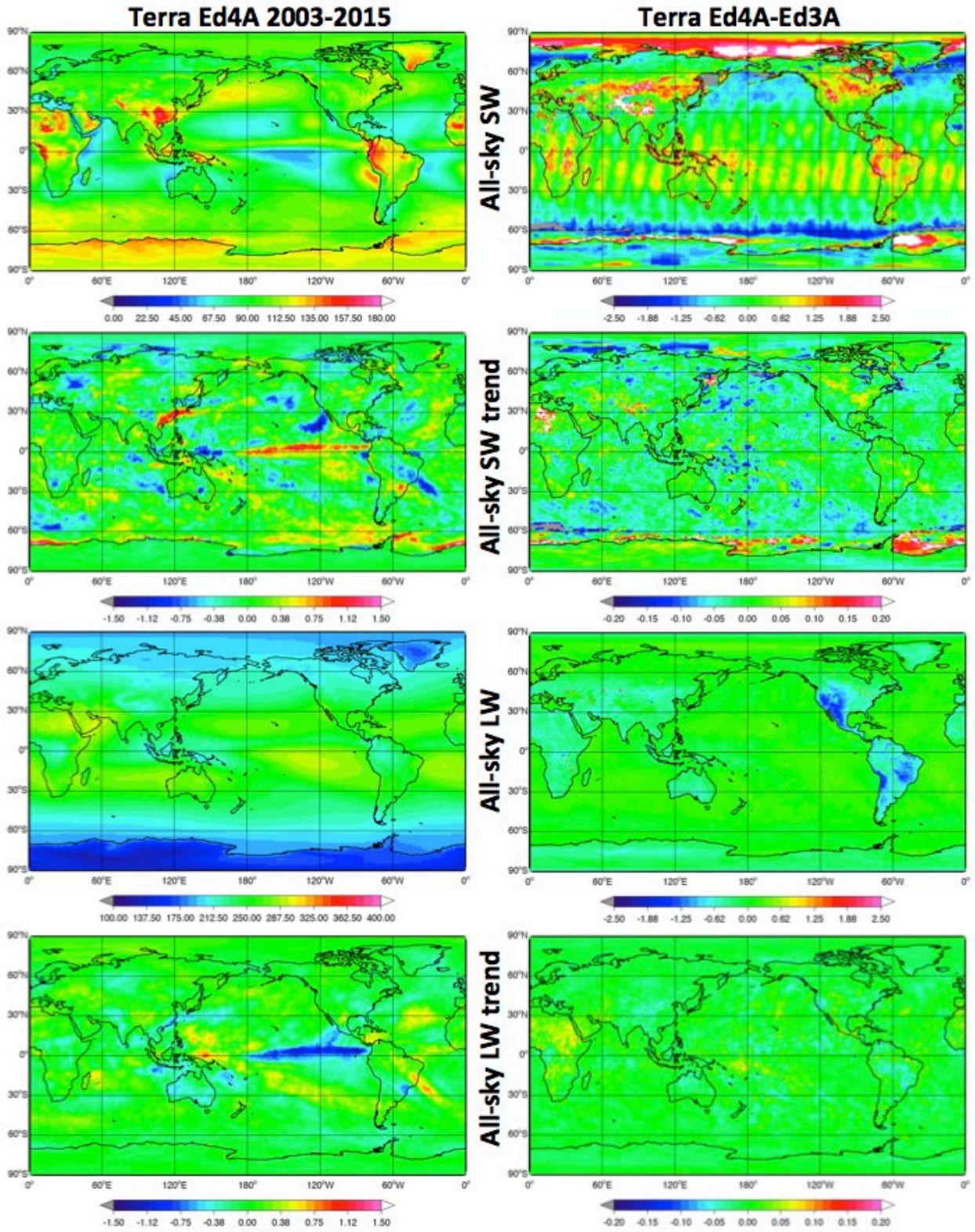

Figure 5-3. The Terra 2003-2015 13-year regional means of (left panel) SSF1deg Ed4A and (right panel) Ed4A minus Ed3A for (top row) all-sky SW flux, (2nd row) all-sky SW flux trend, (3rd row) all-sky LW flux, and (bottom row) all-sky LW flux trend. Unit of flux is W m^{-2}; unit of flux trend is W m^{-2} yr^{-1}.

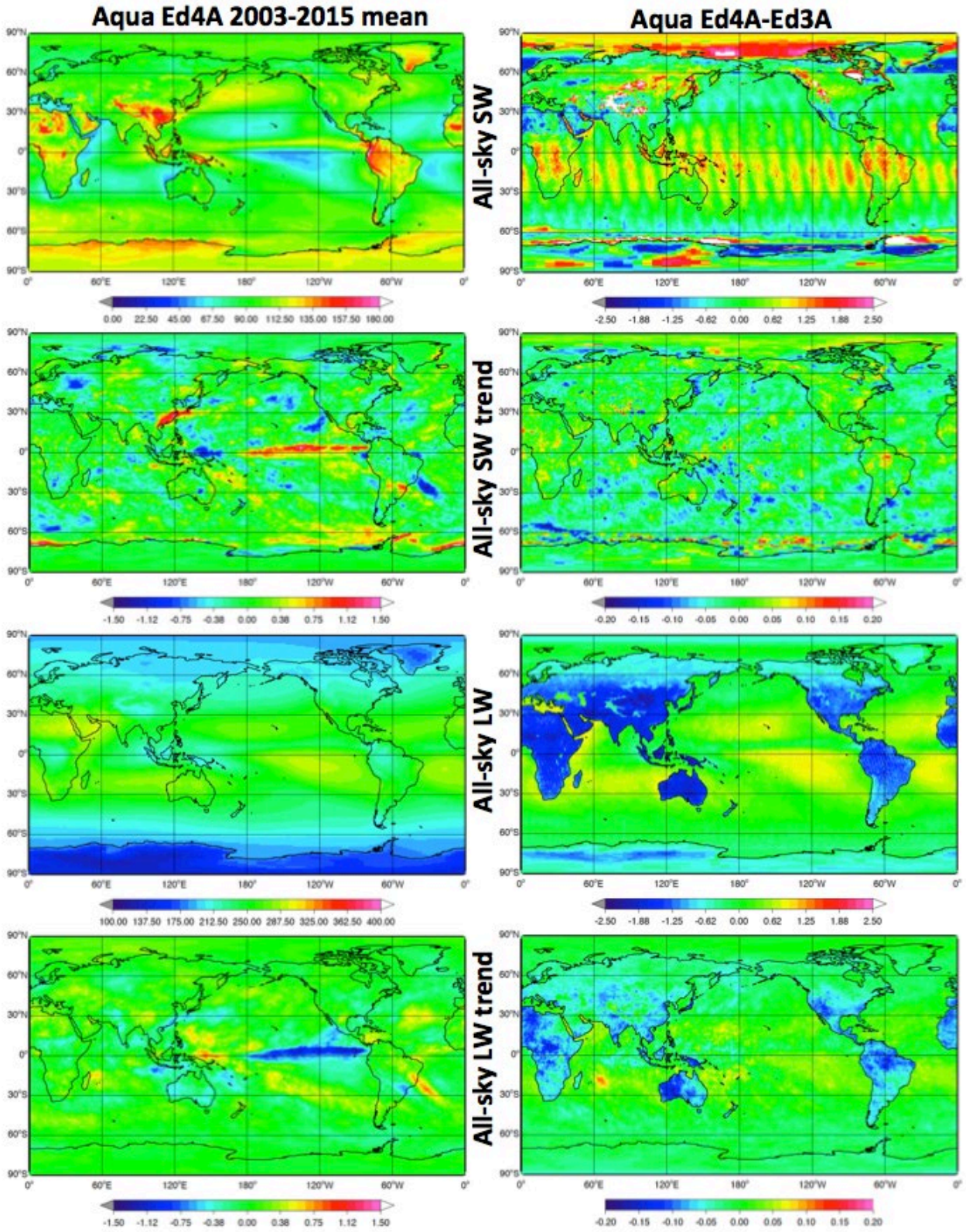

Figure 5-4. Same as Figure 5-3, except for Aqua.

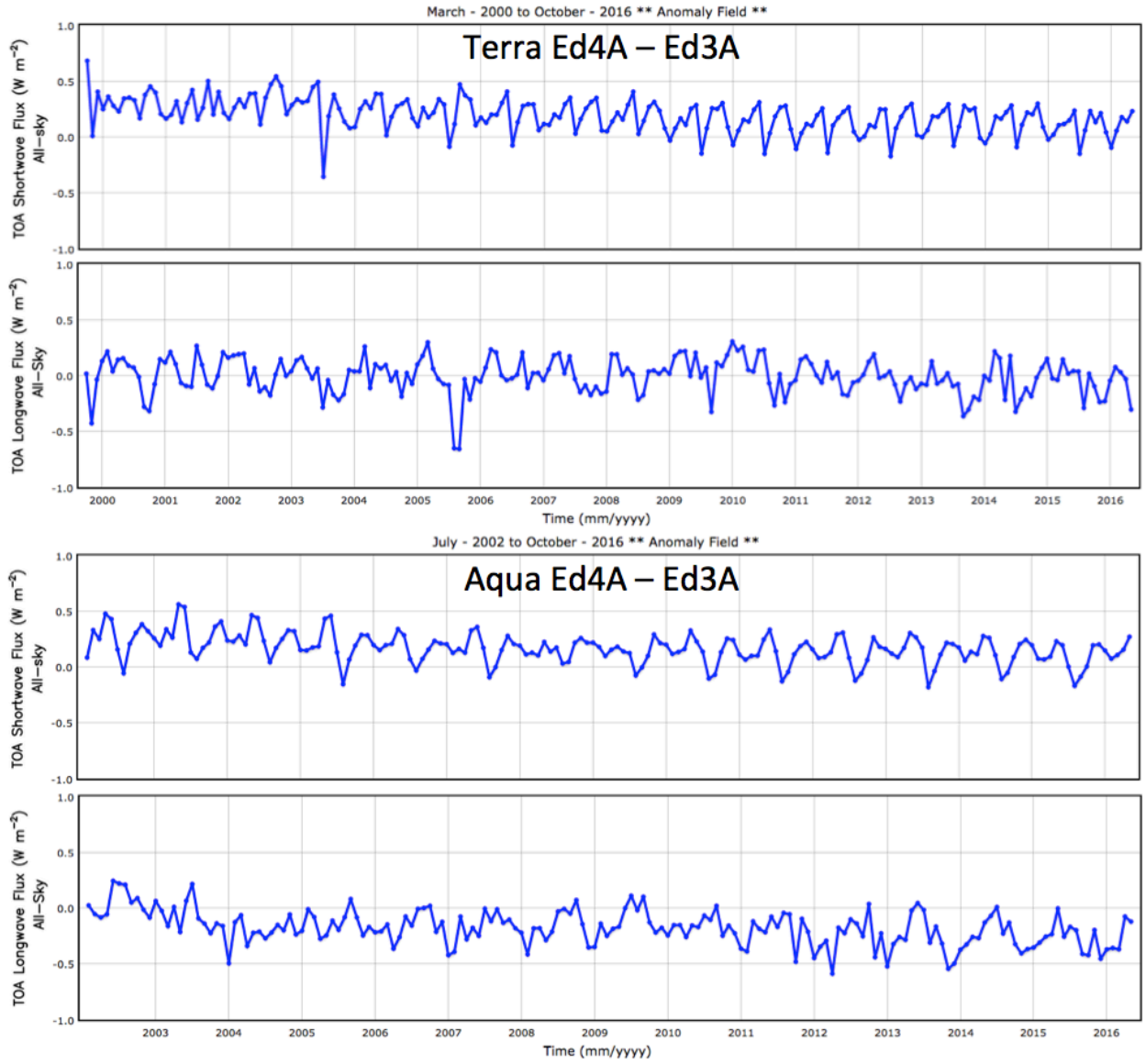

Figure 5-5. The global monthly mean SSF1deg Ed4A minus Ed3A for (top panel) Terra all-sky SW flux, (2nd panel) Terra all-sky LW flux, (3rd panel) Aqua all-sky SW flux, and (bottom panel) Aqua all-sky LW flux. Units in W m^{-2}.

Figure 5-6 shows the clear-sky LW and SW regional flux Ed4A minus Ed3A differences. The differences are associated with the increase of cloud fraction shown in Figure 5-1. For LW the high thin cloud increase near the ITCZ has removed the clear-sky-identified LW fluxes that were in the Ed3A product. The polar sea ice LW clear-sky fluxes have also increased from reducing the clear-sky fraction and reducing frequency of cloud contamination from Ed3A. The Ed4A clear-sky SW increased over the sea ice near Antarctica, since the cloud mask can successfully detect clear-sky over sea ice better than the Ed3A Terra product.

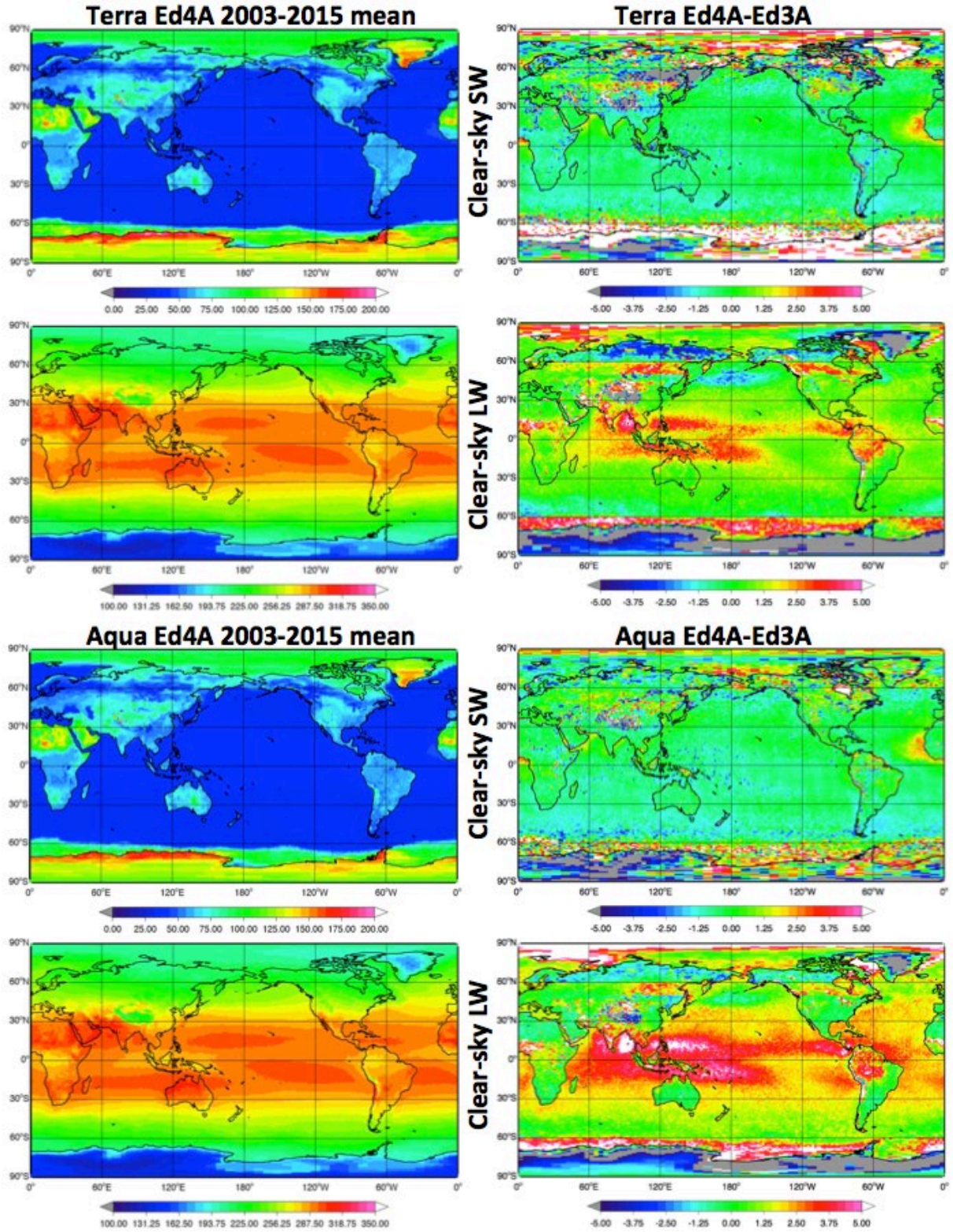

Figure 5-6. The 2003-2015 13-year regional means of (left panel) SSF1deg Ed4A and (right panel) Ed4A minus Ed3A for (top row) Terra clear-sky SW flux, (2nd row) Terra clear-sky LW flux, (3rd row) Aqua clear-sky SW flux, and (bottom row) Aqua clear-sky LW flux. Units in W m^{-2}.

Table 5-2 shows the 2003 to 2015 global mean all-sky and clear-sky SW, LW, and net fluxes for both satellites and for Ed3A and Ed4A. The Ed4A minus Ed3A SW all-sky differences are very small, ~0.17 W m^{-2}; the LW all-sky difference is near zero for Terra and ~ -0.2 W m^{-2} for Aqua. The Terra and Aqua global mean flux differences are mainly associated with the difference in local equator crossing times between Terra (10:30AM) and Aqua (1:30PM), since the Terra and Aqua CERES instruments have been radiometrically scaled. The Ed4A cloud algorithm has reduced the frequency of cloud contamination, thereby decreasing the clear-sky SW flux from Ed3A for Terra and making it more consistent with the Aqua SW clear-sky flux. The clear-sky LW flux for Terra and Aqua has increased by 0.7 W m^{-2} and 1.5 W m^{-2}, respectively. This is in line with the Ed4A cloud mask removing high thin clouds more effectively. Unlike the EBAF product, the clear-sky regions are not spatially complete. The clear-sky global average is based on the sparse spatial sampling of the CERES observed clear-sky footprints. Therefore, the clear-sky net flux may not equal the traditional definition of net flux (Net = Solar incoming (S_0) - SW - LW) as the all-sky net fluxes do.

Table 5-2. The 2003-2015 13-year global mean TOA solar incoming (S_0), SW, LW and net fluxes (W m^{-2}) for all-sky and clear-sky from CERES Terra and Aqua SSF1deg Ed3A and Ed4A.

Dataset (W m^{-2})	All-sky				Clear-sky		
SSF1deg	S_0	SW	LW	Net	SW	LW	Net
Terra Ed3A	339.98	96.21	239.26	4.52	51.28	267.44	21.04
Terra Ed4A	339.98	96.38	239.25	4.35	50.58	268.15	20.89
Aqua Ed3A	339.98	96.02	239.01	4.96	50.02	267.34	22.49
Aqua Ed4A	339.98	96.19	238.83	4.97	49.79	268.79	20.78

5.3 Initial SSF1deg Ed4A Terra, Aqua, and NPP Comparisons

The NPP SSF1deg Ed1A data uses algorithms that are identical to those used in the Aqua and Terra SSF1deg Ed4A production. However, the initial NPP SSF1deg Ed1A CERES instrument calibration has not been radiometrically scaled to be consistent with the Terra and Aqua instrument calibration. The NPP SSF1deg Ed1A product incorporates VIIRS imager cloud properties that may differ from the MODIS cloud properties. Any difference in cloud properties may also impact the fluxes. Also, differences between the MODIS and VIIRS cloud masks may cause differences in the clear-sky fluxes. The NPP Ed1A ADMs use the same Aqua MODIS Ed4A ADMs.

Table 5-3 shows the December 2012 to November 2015 Terra, Aqua, and NPP global mean SW and LW all-sky and clear-sky fluxes for Ed4A. A quick look at the global mean differences indicates that the NPP CERES instrument SW calibration is brighter than Aqua or Terra. This is confirmed by the CERES instrument group; four years of observed Aqua and NPP CERES footprint matched fluxes indicate that NPP is brighter by 1.5% (https://ceres.larc.nasa.gov/documents/STM/2016-04/3_IWGstatus_CERES_Spring16_SThomas.pdf). Also, the NPP clear-sky LW is 1% and 0.2% warmer than Terra and Aqua, respectively. The CERES team is analyzing the differences and

making the necessary calibration, cloud property, and ADM improvements to provide consistent Aqua and NPP records of the CERES fluxes for the future NPP Ed2A product and for a seamless transition between Aqua and NPP.

Table 5-3. The December 2012 to November 2015 3-year global mean TOA solar incoming (S_0), SW, LW and net fluxes (W m^{-2}) for all-sky and clear-sky from CERES Terra and Aqua SSF1deg Ed4A and NPP SSF1deg Ed1A products.

Dataset (W m^{-2})	**All-sky**				**Clear-sky**		
SSF1deg	**S_0**	**SW**	**LW**	**Net**	**SW**	**LW**	**Net**
Terra Ed4A	340.07	96.29	239.28	4.50	50.56	268.06	21.10
Aqua Ed4A	340.07	96.05	238.96	5.05	49.81	268.70	21.00
NPP Ed1A	340.07	97.58	238.22	4.27	50.80	269.16	18.93

6.0 References

Collins, W. D., P. J. Rasch, B. E. Eaton, B. V. Khattatov, J.-F. Lamarque, and C. S. Zender, 2001: Simulating aerosols using a chemical transport model with assimilation of satellite aerosol retrievals: Methodology for INDOEX. *J. Geophys. Res*., **106**, 7313–7336, doi:10.1029/2000JD900507.

Doelling, D. R., N. G. Loeb, D. F. Keyes, M. L. Nordeen, D. Morstad, C. Nguyen, B. A. Wielicki, D. F. Young, and M. Sun, 2013: Geostationary enhanced temporal interpolation for CERES flux products. *J. Atmos. Oceanic Technol*., **30**, 1072-1090.

Doelling, D. R., M. Sun, L. T. Nguyen, M. L. Nordeen, C. O. Haney, D. F. Keyes, and P. E. Mlynczak, 2016: Advances in geostationary-derived longwave fluxes for the CERES Synoptic (SYN1deg) product, *J. Atmos. Oceanic Technol*. **33**, 503-521, doi: 10.1175/JTECH-D-15-0147.1.

Johnson, G. C., J. M. Lyman, and N. G. Loeb, 2016: Improving estimates of Earth's energy imbalance. *Nat. Clim. Change*, **6**, 639-640, doi:10.1038/nclimate3043.

Kato, S., and N. G. Loeb, 2003: Twilight irradiance reflected by the earth estimated from Clouds and the Earth's Radiant Energy System (CERES) measurements. *J. Climate*, **16**, 2646–2650.

Kato, S., and N. G. Loeb, 2005: Top-of-atmosphere shortwave broadband observed radiance and estimated irradiance over polar regions from Clouds and the Earth's Radiant Energy System (CERES) instruments on Terra, *J. Geophys. Res*., **110**, D07202, doi:10.1029/2004JD005308.

Kato, S., F. G. Rose, and T. P. Charlock, 2005: Computation of domain-averaged irradiance using satellite-derived cloud properties. *J. Atmos. Oceanic Technol.,* **22**, 146–164, doi: 10.1175/JTECH-1694.1.

Kopp, G., G. Lawrence, and G. Rottman, 2005: The Total Irradiance Monitor (TIM): Science Results, *Sol. Phys.*, **230**, 129-140.

Loeb, N. G., K. J. Priestley, D. P. Kratz, E. B. Geier, R. N. Green, B. A. Wielicki, P. O. R. Hinton, and S. K. Nolan, 2001: Determination of unfiltered radiances from the Clouds and the Earth's Radiant Energy System (CERES) instrument. *J. Appl. Meteor*., **40**, 822–835.

Loeb, N. G., N. M. Smith, S. Kato, W. F. Miller, S. K. Gupta, P. Minnis, and B. A. Wielicki, 2003: Angular distribution models for top-of-atmosphere radiative flux estimation from the Clouds and the Earth's Radiant Energy System instrument on the Tropical Rainfall Measuring Mission Satellite. Part I: Methodology. *J. Appl. Meteor*., **42**, 240–265.

Loeb, N. G., S. Kato, K. Loukachine, and N. M. Smith, 2005: Angular distribution models for top-of-atmosphere radiative flux estimation from the Clouds and the Earth's Radiant Energy System instrument on the Terra satellite. Part I: Methodology. *J. Atmos. Oceanic Technol.*, **22**, 338–351.

Loeb, N. G., S. Kato, K. Loukachine, and N. Manalo-Smith, 2007: Angular distribution models for top-of-atmosphere radiative flux estimation from the Clouds and the Earth's Radiant Energy System instrument on the Terra satellite. Part II: Validation. *J. Atmos. Oceanic Technol.*, **24**, 564–584.

Loeb, N. G., B. A. Wielicki, D. R. Doelling, G. L. Smith, D. F. Keyes, S. Kato, N. Manalo- Smith, T. Wong, 2009: Toward optimal closure of the Earth's top-of-atmosphere radiation budget. *J. Climate*, **22**, 748-766, doi:10.1175/2008JCLI2637.1.

Loeb, N. G., N. Manalo-Smith, W. Su, M. Shankar, and S. Thomas, 2016: CERES top-of-atmosphere earth radiation budget climate data record: accounting for in-orbit changes in instrument calibration. *Remote Sens.*, **8**(3), 182, doi:10.3390/rs8030182.

Minnis, P., D. R. Doelling, L. Nguyen, W. F. Miller, and V. Chakrapani, 2008: Assessment of the visible channel calibrations of the TRMM VIRS and MODIS on Aqua and Terra, *J. Atmos. Oceanic Technol.*, **25**, 385-400, doi: 10.1175/2007JTECHA1021.1

Minnis P., S. Sun-Mack, D. F. Young, P. W. Heck, D. P. Garber, Y. Chen, D. A. Spangenberg, R. F. Arduini, Q. Z. Trepte, W. L. Smith, Jr., J. K. Ayers, S. C. Gibson, W. F. Miller, G. Hong, V. Chakrapani, Y. Takano, K.-N. Liou, Y. Xie, and P. Yang, 2011: CERES Edition-2 cloud property retrievals using TRMM VIRS and Terra and Aqua MODIS data--Part I: Algorithms. *IEEE Trans. Geosci. Remote Sens.*, **49**, 4374-4400.

Remer, L. A., and Coauthors, 2005: The MODIS aerosol algorithm, products, and validation. *J. Atmos. Sci.*, **62**, 947–973, doi:10.1175/JAS3385.1.

Rienecker, M., and Coauthors, 2008: The GEOS-5 data assimilation system—Documentation of versions 5.0.1, 5.1.0, and 5.2.0. M. J. Suarez, Ed., Tech. Rep. Series on Global Modeling and Data Assimilation, Vol. 27, NASA Tech. Memo. NASA/TM- 2008-104606, 101 pp.

Roemmich, D. et al., 2009: Argo: the challenge of continuing 10 years of progress. *Oceanography*, **22**, 46–55, doi:10.5670/oceanog.2009.65.

Su, W., J. Corbett, Z. A. Eitzen, and L. Liang, 2015a: Next-generation angular distribution models for top-of- atmosphere radiative flux calculation from the CERES instruments: Methodology. *Atmos. Meas. Tech*., **8**, 611–632.

Su, W., J. Corbett, Z. A. Eitzen, and L. Liang, 2015b: Next-generation angular distribution models for top-of- atmosphere radiative flux calculation from the CERES instruments: Validation. *Atmos. Meas. Tech*., **8**, 3297–3313.

Thomas, S., K. J. Priestley, N. Manalo-Smith, N. G. Loeb, P. C. Hess, M. Shankar, D. R. Walikainen, Z. P. Szewcyzk, R. S. Wilson, D. L. Cooper, 2010: Characterization of the Clouds and the Earth's Radiant Energy System (CERES) sensors on the Terra and Aqua spacecraft, Proc. SPIE, Earth Observing Systems XV, Vol. 7807, 780702, August 2010.

Wu, A., X. Xiong, D.R. Doelling, D. Morstad, A. Angal, and R. Bhatt, 2013: Characterization of Terra and Aqua MODIS VIS, NIR and SWIR Spectral Bands Calibration Stability, *IEEE Trans. Geosci. Remote Sens*., **51**, 4330-4338, doi:10.1109/TGRS.2012.2226588.

Young, D. F., P. Minnis, D. R. Doelling, G. G. Gibson, and T. Wong, 1998: Temporal Interpolation Methods for the Clouds and Earth's Radiant Energy System (CERES) Experiment. *J. Appl. Meteorol*., **37**, 572-590.

7.0 Expected Reprocessing

There are no plans to reprocess the SSF1deg Ed4A record until the CERES Edition 5 suite of data products are available. Any updates to the CERES SSF1deg products will be available for subsetting/visualization/ordering at: https://ceres.larc.nasa.gov/data/.

8.0 Attribution

When referring to the CERES SSF1deg product, please include the product and data set version as: “CERES Terra SSF1deg Ed4A,” “CERES Aqua SSF1deg Ed4A,” “CERES NPP SSF1deg Ed2A.,” or “CERES NOAA-20 SSF1deg Ed1B.”

The CERES Team has put forth considerable effort to remove major errors and to verify the quality and accuracy of this data. Please provide a reference to the following paper when you publish scientific results with the CERES Terra/Aqua SSF1deg Edition4A, NPP SSF1deg Edition2A, or NOAA-20 SSF1deg Edition1B products:

Wielicki, B. A., B. R. Barkstrom, E. F. Harrison, R. B. Lee III, G. L. Smith, and J. E. Cooper, 1996: Clouds and the Earth's Radiant Energy System (CERES): An Earth Observing System Experiment, *Bull. Amer. Meteor. Soc.*, **77**, 853-868.

The CERES data products now have DOIs. To cite the data in a publication, use this format:

CERES Science Team, Hampton, VA, USA: NASA Atmospheric Science Data Center (ASDC), Accessed <**author citing data inserts date here**> at doi: (appropriate product)

For SSF1deg-Hour:
- 10.5067/Aqua/CERES/SSF1degHour_L3.004
- 10.5067/Terra/CERES/SSF1degHour_L3.004
- 10.5067/NPP/CERES/SSF1degHour_L3.002A
- 10.5067/NOAA20/CERES/SSF1degHour_L3.001B

For SSF1deg-Day:
- 10.5067/Aqua/CERES/SSF1degDay_L3.004A
- 10.5067/Terra/CERES/SSF1degDay_L3.004
- 10.5067/NPP/CERES/SSF1degDay_L3.002A
- 10.5067/NOAA20/CERES/SSF1degDay_L3.001B

For SSF1deg-Month:
- 10.5067/Aqua/CERES/SSF1degMonth_L3.004A
- 10.5067/Terra/CERES/SSF1degMonth_L3.004A
- 10.5067/NPP/CERES/SSF1degMonth_L3.002A
- 10.5067/NOAA20/CERES/SSF1degMonth_L3.001B

When Langley ASDC data are used in a publication, we request the following acknowledgment be included: "These data were obtained from the NASA Langley Research Center Atmospheric Science Data Center." The Langley ASDC requests a reprint of any published papers or reports or a brief description of other uses (e.g., posters, oral presentations, etc.) of data that we have distributed. This will help us determine the use of data that we distribute, which is helpful in optimizing product development. It also helps us to keep our product related references current.

When CERES data obtained via the CERES web site are used in a publication, we request the following acknowledgment be included: “These data were obtained from the NASA Langley Research Center CERES ordering tool at https://ceres.larc.nasa.gov/data/.”

9.0 Feedback and Questions

For questions or comments on this CERES SSF1deg Hour/Day/Month Data Quality Summary, contact the User and Data Services staff at the Atmospheric Science Data Center.

For questions about the CERES subsetting/visualization/ordering tool at https://ceres.larc.nasa.gov/data/, please email LaRC-CERES-Help@mail.nasa.gov.

10.0 Appendix - The Calendar Year Anomaly Dilemma

The CERES SSF1deg-Hour/Day/Month Ed4A products are based on GMT calendar days and months. The actual number of days for the Earth to orbit the sun is 365.256 days because the Earth's rotation about the axis or spin rate is not synchronized with the time it takes for the Earth to orbit the sun. Performing monthly deseasonalization or annual anomalies based on the calendar year may introduce unwanted variability when interpreting CERES fluxes. This would not be the case if the definition of the year were 365.256 days and if the 12 months were exactly divided into 30.4375 days. Care must be taken when interpreting monthly flux anomalies. This section illustrates some of the common unintended flux anomalies that stem from using the calendar month and year.

The calendar year anomalies can be mitigated using 4-year running means or 4-year averages when evaluating solar incoming and SW fluxes. For analyzing long-term datasets this is necessary. However, when analyzing small scale short-term SW flux variability, the calendar-induced oscillations should be much smaller than the natural variability.

CERES SSF1deg Ed4A products are based on hourly updated ephemeris data of declination angle, Earth-sun distance, and sidereal day correction. These annual oscillations are shown in Figure 10-1. The Consultative Committee for Space Data Systems (CCSDS) 301.0-B-2 Astronomical Almanac ephemeris data are used to compute solar angles and are available in the SDP toolkit for the EOSDIS Core System Project (https://newsroom.gsfc.nasa.gov/sdptoolkit/toolkit.html).

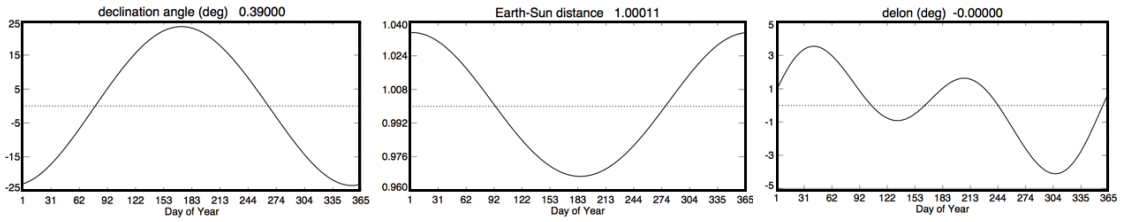

Figure 10-1. (left) The Earth's declination angle (deg), (middle) Earth-sun distance correction factor, and (right) sidereal day angle or equation of time (deg) as a function of day of year.

The first example of a calendar year induced anomaly is taking the solar incoming anomaly. The CERES Edition 4 solar irradiance is from SORCE that is updated daily (SORCE Level 3 Total Solar Irradiance Version 15 available from https://lasp.colorado.edu/data/tsis/tsi_data/tsis_tsi_L3_c24h_latest.txt). The SORCE total solar irradiance (TSI) is ~1361 W m^{-2}. After subtracting the record mean the SORCE TSI anomaly will vary over the sunspot cycle with an amplitude of ~0.1% over ~11 years as shown in Figure 10-2 (left panel, red line). The black line shows the calendar monthly anomaly of the global solar incoming with oscillations on the order of 0.05 W m^{-2}. Now suppose I have daily Earth-Sun distance correction factors for 3 years based on a 365-day year and 1 year based on a 366-day year. For simplicity, I assume that the TSI is constant at 1361 W m^{-2}. Now I take the calendar monthly anomaly of the global solar incoming flux and plot it in Figure 10-2 (right panel). Clearly, the leap

year is causing the ~1.25 oscillations per year with a 0.1 W m^{-2} amplitude. The oscillations are due to the small difference in aligning the Earth-Sun distance from year to year. Figure 10-3 shows the solar incoming anomaly over four zonal bands. Over the tropics the TSI 11-year cycle is apparent. However, the zones near the polar latitudes plainly show leap year patterns, where the magnitude of the calendar year induced anomaly can be as large as 3 W m^{-2} for 75° to 80° N.

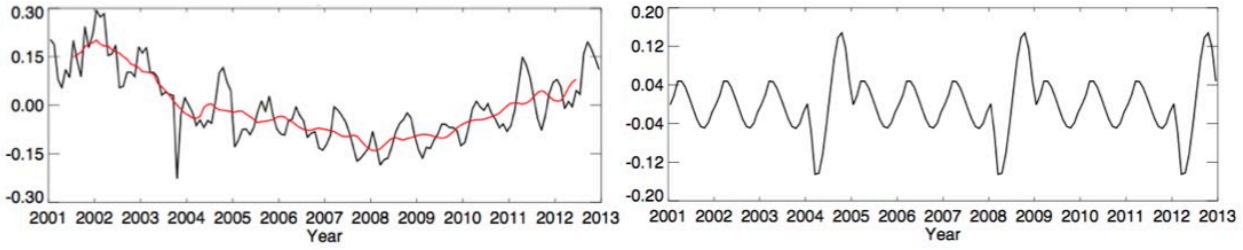

Figure 10-2. (left) The monthly SSF1deg Ed4A total solar incoming (TSI) irradiance anomaly based on the calendar year (black line) and the monthly SORCE TSI anomaly after subtracting the record mean (red line). (right) The theoretical monthly TSI anomaly based on a solar constant of 1361 W m^{-2} and the calendar year. Units in W m^{-2}.

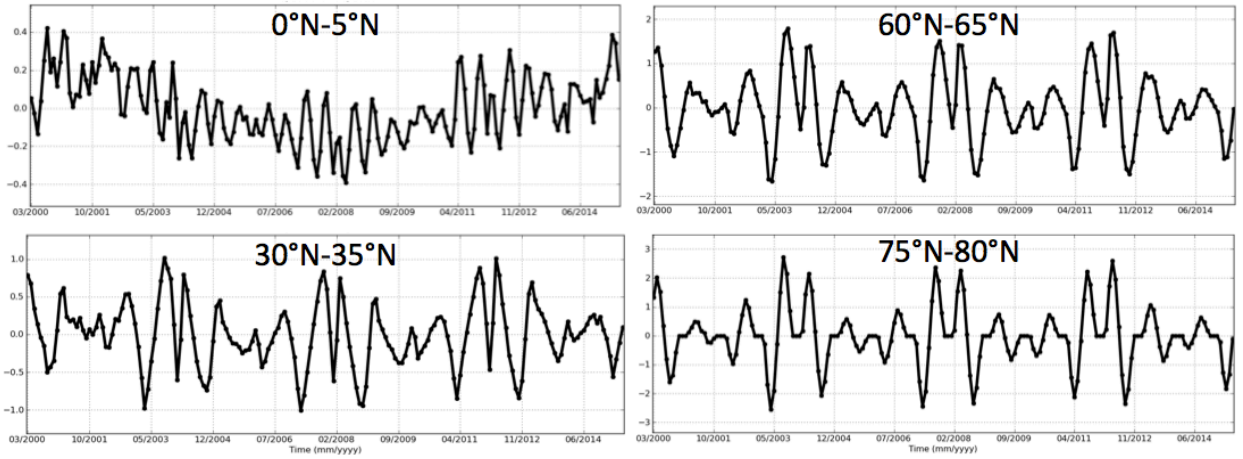

Figure 10-3. The SSF1deg Ed4A zonal monthly TSI anomalies for 4 latitude zones. Units in W m^{-2}.

The second example of a calendar year induced anomaly is performing southern minus northern hemisphere annual global mean solar incoming flux differences. Table 10-1 shows the difference using a calendar year and a 365.25-day year. When using a 365.25-day year the solar incoming hemisphere difference annual variability is limited to ~0.02 W m^{-2}. However, when using a calendar year, the non-leap year hemisphere difference is ~ -0.2 W m^{-2} and during the leap year the hemisphere difference is +0.6 W m^{-2}. The calendar year induced anomaly of the hemispheric solar incoming flux difference is ~0.8 W m^{-2}, much larger than the true hemispheric flux difference, which is nearly balanced.

Table 10-1. The annual Southern minus Northern Hemisphere TSI flux difference (W m^{-2}) as a function of a 365.25-day year and a calendar year. Note that 2004 is a leap year with 366 days.

SH-NH TSI Year	365.25-Day Year	Calendar Year
2001	0.027	-0.162
2002	0.029	-0.160
2003	0.012	-0.178
2004	0.019	+0.585

Lastly, when computing the annual mean from monthly data, the most accurate way is to weight by the number of days during each month. Not weighting the monthly solar incoming can cause a bias of 0.04 W m^{-2} in deriving the annual mean (Table 10-2). Also, not weighting by the number of days of the months can cause 4-year oscillations in the solar incoming of 0.02 W m^{-2}. Examples of the annual means of SW and LW flux are also shown in Table 10-2.

Table 10-2. The monthly weighted minus daily weighted global annual SW, LW, and solar incoming flux (W m^{-2}). Note that 2004 and 2008 are leap years.

Year	SW	LW	Solar
2003	0.015	-0.018	0.044
2004	0.000	-0.005	0.021
2005	0.019	-0.013	0.043
2006	0.014	-0.019	0.043
2007	0.008	-0.013	0.044
2008	0.013	-0.006	0.020

11.0 Document Revision Record

The Document Revision Record contains information pertaining to approved document changes. The table lists the Version Number, the date of the last revision, a short description of the revision, and the revised sections.

Document Revision Record

Version Number	Date	Description of Revision	Section(s) Affected
V1	08/09/2021	• Existing document put in version control.	All
V2	08/04/2023	• Added data outage, drift, and RAPS information. • Added NPP and NOAA-20 to the CERES instrument radiometric scaling bullet. • Added NOAA-20 cloud property information. • Updated DOIs.	Section 3.0 Section 8.0